AD-A154 102 DEVELOPMENT OF THE TACOM (TANK AUTOMOTIVE COMMAND) THERMAL IMAGING MODEL (.. (U) OPTIMETRICS INC ANN ARBOR MI T J ROGNE ET AL. DEC 84 TACOM-TR-13081-VOL-1 1/1

UNCLASSIFIED DAAE07-81-C-4053 F/G 17/5 NL

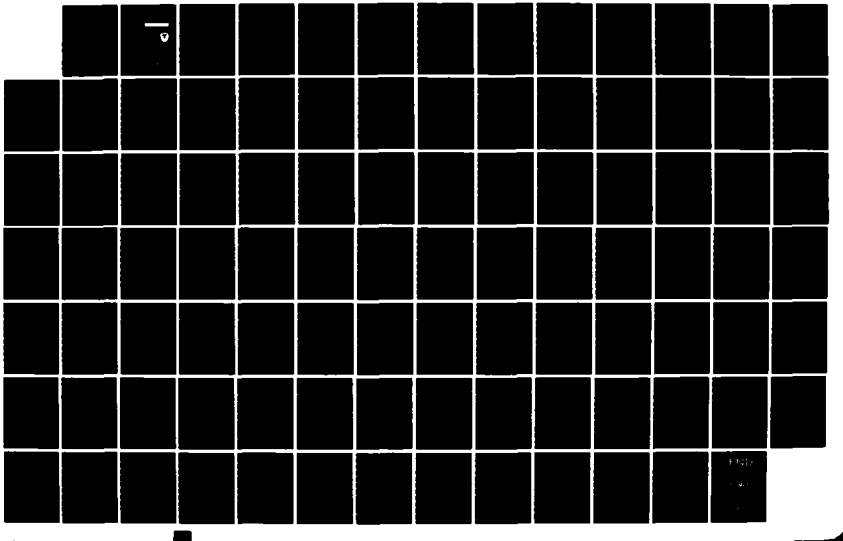

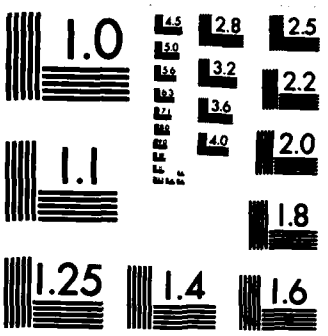

R and D CENTER LABORATORY

TECHNICAL REPORT

NO. 13081

DEVELOPMENT OF THE TACOM THERMAL IMAGING MODEL

TECHNICAL GUIDE AND USER'S MANUAL

(Volume I)

Contract # DAAE07-81-C-4053

December 1984

by TIMOTHY J. ROGNE
BRIAN K. MATISE
FREDERICK G. SMITH
OPTIMETRICS, INC.
2000 Hogback Road, Suite 3
Ann Arbor, MI 48104

APPROVED FOR PUBLIC RELEASE:
DISTRIBUTION UNLIMITED

U.S. ARMY TANK-AUTOMOTIVE COMMAND
RESEARCH AND DEVELOPMENT CENTER
Warren, Michigan 48090

UNCLASSIFIED
SECURITY CLASSIFICATION OF THIS PAGE

REPORT DOCUMENTATION PAGE

1a. REPORT SECURITY CLASSIFICATION UNCLASSIFIED	1b. RESTRICTIVE MARKINGS NONE
2a. SECURITY CLASSIFICATION AUTHORITY	3. DISTRIBUTION/AVAILABILITY OF REPORT APPROVED FOR PUBLIC RELEASE: DISTRIBUTION UNLIMITED
2b. DECLASSIFICATION/DOWNGRADING SCHEDULE	
4. PERFORMING ORGANIZATION REPORT NUMBER(S)	5. MONITORING ORGANIZATION REPORT NUMBER(S)
6a. NAME OF PERFORMING ORGANIZATION OPTIMETRICS, INC. — 6b. OFFICE SYMBOL (If applicable)	7a. NAME OF MONITORING ORGANIZATION
6c. ADDRESS (City, State, and ZIP Code) ANN ARBOR, MI 48104	7b. ADDRESS (City, State, and ZIP Code)
8a. NAME OF FUNDING/SPONSORING ORGANIZATION Survivability Research Div — 8b. OFFICE SYMBOL (If applicable) AMSTA-ZS	9. PROCUREMENT INSTRUMENT IDENTIFICATION NUMBER DAAE07-81-C-4053
8c. ADDRESS (City, State, and ZIP Code) US Army TACOM, TACL, Bldg 200C Warren, MI 48397-5000	10. SOURCE OF FUNDING NUMBERS PROGRAM ELEMENT NO. — PROJECT NO. — TASK NO. — WORK UNIT ACCESSION NO.

11. TITLE (Include Security Classification)
Development of the TACOM Thermal Imaging Model (TTIM) - Volume I

12. PERSONAL AUTHOR(S)
Timothy J. Rogne, Brian K. Matise, Frederick G. Smith

13a. TYPE OF REPORT	13b. TIME COVERED	14. DATE OF REPORT (Year, Month, Day)	15. PAGE COUNT
Final	FROM Jun 84 TO Dec 84	84 Dec	90

16. SUPPLEMENTARY NOTATION

17. COSATI CODES			18. SUBJECT TERMS (Continue on reverse if necessary and identify by block number)
FIELD	GROUP	SUB-GROUP	FLIR Modeling ; Thermal Imaging System Modeling ; Image Simulation .

19. ABSTRACT (Continue on reverse if necessary and identify by block number)

This report describes TACOM's Thermal Imaging Model (TTIM). The model allows measured or modeled scenes to be viewed by a simulated imaging sensor. The resulting scene is then displayed for observer evaluation. Currently, the model is operating on a Digital Equipment Corporation VAX 11/750 at US Army Tank-Automotive Command in Warren, MI.

20. DISTRIBUTION/AVAILABILITY OF ABSTRACT	21. ABSTRACT SECURITY CLASSIFICATION
☒ UNCLASSIFIED/UNLIMITED ☐ SAME AS RPT. ☐ DTIC USERS	UNCLASSIFIED
22a. NAME OF RESPONSIBLE INDIVIDUAL JAMES M. GRAZIANO, GRANT R. GERHART	22b. TELEPHONE (Include Area Code) (313) 574-8634 — 22c. OFFICE SYMBOL AMSTA-ZSA

DD FORM 1473, 84 MAR — 83 APR edition may be used until exhausted. All other editions are obsolete.

SECURITY CLASSIFICATION OF THIS PAGE
UNCLASSIFIED.

ACKNOWLEDGMENT

The authors would like to acknowledge the cooperation and support of the US Army Tank-Automotive Command (TACOM) and TACOM personnel in the development of this model. Dr. Grant Gerhart conceived the idea for the simulation and initiated the model development. He has also served as the Government's Technical Representative on this project. Dr. James Graziano of TACOM has also assisted in various ways throughout the project. In particular, he has assisted in the installation of the code on the TACOM VAX 11/750 system, with the production of imagery using the TACOM COMTAL image processing system, and with recommendations for improvements in the code.

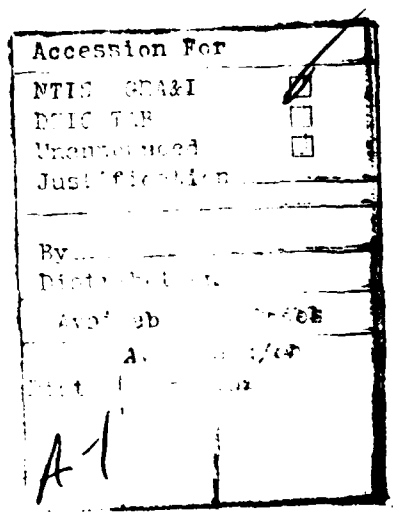

TABLE OF CONTENTS

LIST OF TABLES

LIST OF ILLUSTRATIONS

1.0 Introduction

It has long been recognized that in modeling Electro-Optical sensor performance it is very difficult to account for the ability of a human observer to perform target detection and recognition tasks. In general, our understanding of the human perception process is simply not sufficient to allow for reliable modeling. These facts pose a significant problem for the vehicle and vehicle countermeasure designers at TACOM. Other than the designers' own intuition, little guidance is available concerning the relative detectability of a new vehicle or vehicle countermeasure design. This means that cue features which significantly influence the detectability of a new design may easily pass unnoticed until prototype vehicles are actually constructed and evaluated.

The Imaging Sensor Simulation Model (ISSM) described in this manual represents a step toward alleviating the difficulties associated with predicting the detectability of a concept vehicle design. The model allows the image of a vehicle positioned in an arbitrary background to be displayed as it would be seen if viewed through a simulated sensor under simulated atmospheric conditions. Currently, thermal imaging sensors may be simulated; the atmospheric models include provisions to treat virtually any natural or battlefield obscuration condition. Given a single target/background input image, the model allows the user to vary the observation sensor, viewing range, atmospheric condition, and battlefield scenario. It is hoped that by allowing concept vehicle designs to be viewed in a simulated battlefield environment, the designer will be significantly aided in attempts to create less detectable combat vehicles.

The computer model itself is written in FORTRAN IV so that it may be transported between a wide variety of computer installations. The model is menu driven allowing for convenient operation. Because of the model's large scope, several hundred inputs will commonly be required to specify a single unique calculation. To help manage these inputs, an input library scheme has been implemented so that a number of default sensor, battlefield, and natural atmosphere module input sets can be made available to the user. Selected input sets may then be modified from appropriate user menus.

The model is currently running on an IBM-compatible Amdahl Model 5860 computer system located at the University of Michigan, and a Digital Equipment Corporation VAX 11/750 located at TACOM. The two versions of the model are functionally identical; however, this report specifically treats the TACOM installation.

2.0 Technical Manual

The overall modeling approach is depicted in Figure 2-1. In its principal mode of operation a two-dimensional scene radiance map input to the model is transformed into an image representative of a modeled sensor's output just prior to its display. The units of the input radiance map are W/cm^2-sr-micron; it is assumed that the scene radiance is constant over the spectral bandpass of interest. The output map of sensor signal and noise has units of watts; a voltage map may be obtained by multiplying the output by the modeled sensor responsivity (V/W) should this be desired.

As illustrated in Figure 2-1, the input scene radiance map is allowed to be attenuated by natural or artificial constituents along an atmospheric path. In addition, radiation may be added to the map either due to emission or scattering. The natural atmospheric model is a version of LOWTRAN6 [1] adapted to use in the simulation. The standard version of LOWTRAN6 calculates the attenuation caused by naturally occurring molecular and aerosol species. It also calculates the path radiance due to emission from each species, and aerosol scattering of point source (eg. solar) radiation. It is assumed that natural atmospheric effects will be spatially uniform across the entire image. Further, the spectral variations in the atmospheric path radiance and attenuation are averaged over the bandpass of interest prior to modifying the input scene radiance map.

The battlefield effects model is a modified version of the ACTMAD [2] computer code. This model was developed by OptiMetrics for the US Army Atmospheric Sciences Laboratory (ASL). The code combines the ASL smoke model ACT II [3] with the OptiMetrics MADPUFF [4,5] smoke model. ACTMAD allows up to 6 varieties of smoke munitions and 12 total smoke sources to be considered simultaneously. The sources may be positioned in any configuration; the model calculates a spatial map of the obscurant cloud attenuation and path radiance. Sky, terrain, and point radiation sources are considered in the path radiance calculation. A notable feature of the ACTMAD model is that it includes (as a user selected option) a statistical turbulent smoke transport and diffusion model. Thus, the modeled smoke clouds can be made to appear more realistically structured than is possible with the more conventional gaussian-type transport and diffusion models.

Because we have calculated the optical properties of the natural and battlefield atmospheres separately, we are faced with the difficulty of combining their effects. To do this,

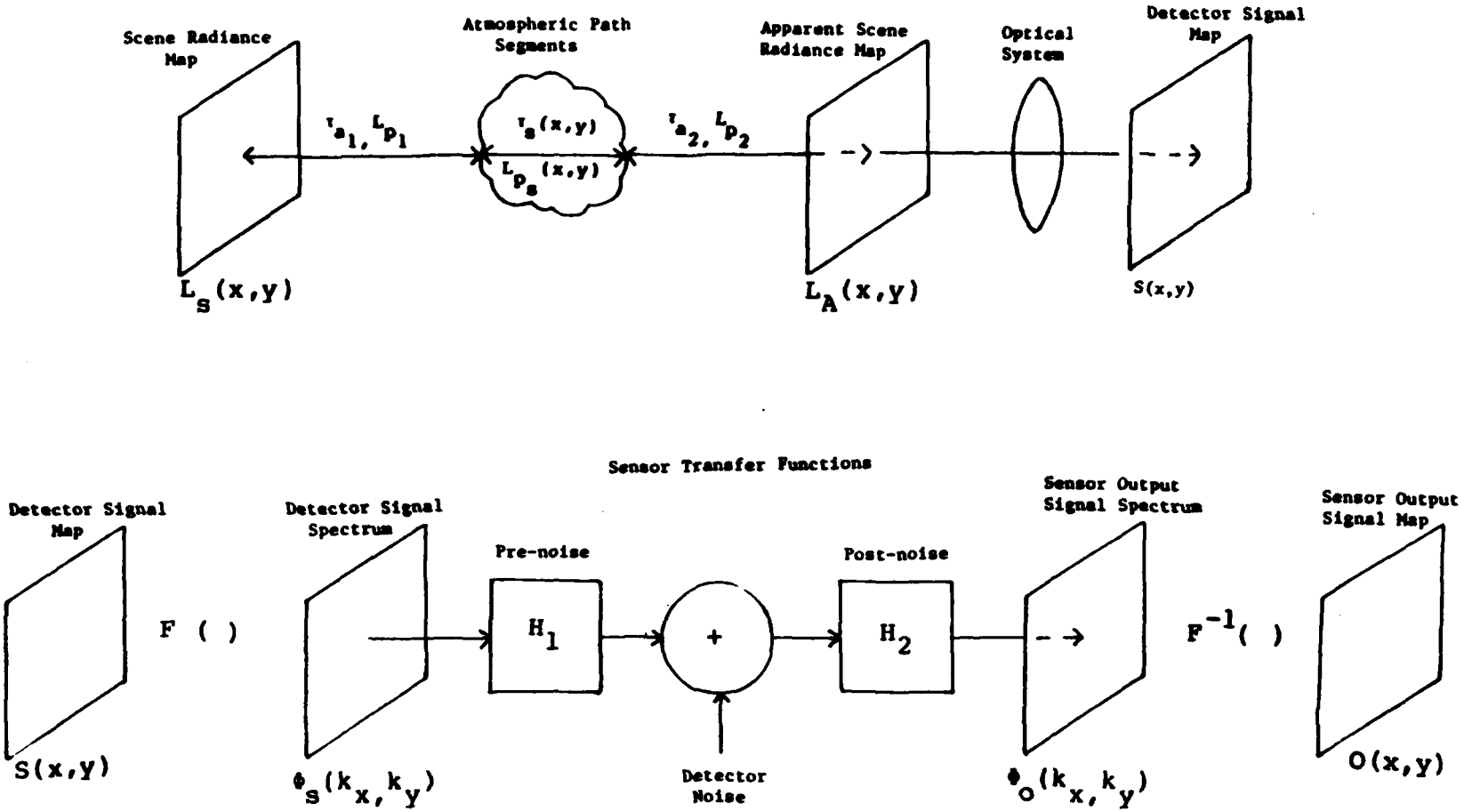

Figure 2-1. Schematic Representation of the Simulation Structure

we make the reasonable assumptions that the obscurant cloud will be localized along the atmospheric path, and that the natural atmospheric effect within an obscurant cloud will be negligible compared with that of the cloud itself. Based on this, the atmospheric path is divided into two segments with the division occurring at the center of the obscurant cloud. The LOWTRAN6 module is used to determine the optical properties of each path. The net path optical properties are then determined according to the following equation:

$$L_A(x,y) = L_{P_2} + L_{P_s}(x,y)\ \tau_{a_2} + L_{P_1}\tau_{a_2}\tau_s(x,y) + L_s(x,y)\ \tau_{a_2}\tau_s(x,y)\ \tau_{a_1} \quad (1)$$

where

L_A = Apparent Scene Radiance Map

$L_{P_{1,2}}$ = Natural Atmosphere Path Radiance from Path Segments 1 and 2 respectively

$\tau_{a_{1,2}}$ = Natural Atmospheric Transmittance along Path Segments 1 and 2 respectively

$\tau_s(x,y)$ = Obscurant Transmittance Map

$L_{P_s}(x,y)$ = Obscurant Path Radiance Map

$L_s(x,y)$ = Scene Radiance Map

The result is a radiance map which represents the input scene as it would appear when viewed from the modeled sensor location.

The sensor model basically consists of two parts. A simple optical system model is used to transform the apparent radiance map into a map of the optical power (watts) from each scene element that contributes to a detector signal. This signal map is then Fourier transformed so that linear transfer functions representing the effect of sensor subsystems may be conveniently applied. White noise is introduced following the sensor detector, and is then filtered by subsequent subsystems. In general, the sensor model utilizes the same subsystem transfer function forms as the NV&EOL Static Performance Model for Thermal Viewing Systems [6]. The most notable exceptions are that display and observer

effects are simulated rather than modeled in our approach. Nevertheless, the sensor descriptions required by the two models are nearly identical and, for simple images such as Minimum Resolvable Temperature (MRT) bar targets, the predictions of the two models should be comparable.

A special capability provided in the model is the ability to perform the inverse of the process described above. In this case, a measured image is input to the model and converted into a scene radiance map. Basically this involves applying the inverse of the measurement sensor transfer functions, subtracting the atmospheric path radiance, and dividing by the atmospheric path transmission.* Unfortunately, the utility of this method is limited by the presence of noise in the measured data, the accuracy to which the measurement sensor can be represented, and the ability to model specific atmospheric conditions.

2.1 Atmospheric Effects Models

Two separate atmospheric effects models (LOWTRAN6 and ACTMAD) are incorporated in the simulation to treat natural and battlefield effects respectively. In the following two subsections we will provide brief descriptions of each model's theoretical basis; however, since both models are fully developed entities in their own right, the reader will be referred to existing technical documentation specific to each model. Our discussion will generally be limited to details peculiar to their implementation in ISSM as well as details which cannot be found in easily obtainable documentation.

2.1.1 Natural Atmospheric Effects Model

The natural atmospheric effects model is an adaptation of the LOWTRAN6 computer code [1] which was developed by the US Air Force Geophysics Laboratory. As suggested by its name, the code is the latest version in a series of atmospheric models developed over the past several years [7, 8, 9, 10].

The LOWTRAN model predicts the transmittance and path radiance for an arbitrary path geometry at a spectral resolution of 20 cm^{-1}. The model normally represents the atmosphere

---

* Note: In the current ISSM version (1.0), we only allow inversion of the sensor transfer functions. This is an oversight which will be corrected in version 2.

using 34 homogeneous layers which describe the vertical profiles of temperature, pressure, water vapor, ozone, and atmospheric aerosols. A number of default vertical profiles are stored with the model; the user may alternatively define a specific model atmosphere using an arbitrary number of layers. In addition to the variable atmospheric quantities, LOWTRAN also treats the so-called uniformly mixed gasses such as CO_2 and N_2O.

Within the spectral range 0.25-28.5 microns, LOWTRAN stores data describing the optical properties of all the naturally occuring gaseous species, and a large number of aerosols including rural haze, urban haze, fog, rain, snow, tropospheric aerosols, and volcanic ash. Using this optical data, LOWTRAN6 calculates the attenuation along an atmospheric path considering the following factors:

- Molecular absorption
- Molecular scattering
- Aerosol absorption
- Aerosol scattering

In calculating the attenuation due to scattering, LOWTRAN assumes that the signal radiation is travelling along a single ray toward a point receiver with an infinitesimal field-of-view. All scattered signal radiation is considered "attenuated"; multiple scattering of radiation is not considered. Therefore, the theoretical possibility that a scattering media may have a non-uniform Modulation Transfer Function (MTF) (that is, that the scattering media may attenuate signal energy at different spatial frequencies with different efficiencies) is not considered by LOWTRAN. It should be noted, however, that there are few if any practical situations involving natural atmospheric effects for which the above consideration is of any significant consequence.

LOWTRAN6 calculates the atmospheric path radiance considering the following factors:

- Molecular emission along the path of interest
- Aerosol emission along the path of interest
- Aerosol single scattering of plane-parallel point sources (eg. solar scattering)

Specifically excluded from consideration are multiply scattered photons, atmospheric emissions scattered into the path of interest, and radiation scattered from extended sources such as the ground. Unfortunately, at the longer infrared wavelengths of interest, the later two effects can be significant. For example, in the 8-12 micron wavelength region, the emissions from the sky and ground hemispheres can easily dominate the contribution from the sun. Therefore, LOWTRAN6 may significantly under-estimate the atmospheric path radiance. As is discussed in section 2.2, this deficiency is of no consequence in the current version of the ISSM since only spatially uniform atmospheric emissions are considered; the linear sensor modeling approach does not consider signal processing dynamic range limitations so that the degradation caused by spatially uniform emissions can always be eliminated by the (modeled) sensor. However, if later versions of the ISSM consider non-uniform atmospheric effects (eg. consideration of the horizon), then the deficiency should be corrected using the ACTMAD radiative transfer modeling techniques (which include the effect of extended sources) discussed in the next section.

2.1.2 Battlefield Effects Model

The ACTMAD [2] battlefield effects model is a derivative of the ACT II [3] smoke obscuration model developed by the US Army Atmospheric Sciences Laboratory (ASL). The ACT II model treats the transport and diffusion of obscurant clouds in a deterministic manner using a gaussian plume methodology. In order to model the spatial and temporal inhomogeneities present in obscurant clouds generated under realistic field conditions, OptiMetrics developed the Microscale Atmospheric Diffusion of Puffs, or MADPUFF methodology. This methodology has been incorporated in the ACT II computer code as a user selected option; the resulting ACTMAD computer code was developed by OptiMetrics for ASL.

2.1.2.1 ACT II Smoke Obscuration Model

The ACT II smoke obscuration effects model [3] allows for the calculation of transmission and path radiance along an arbitrary path through an obscurant cloud. Obscurant sources are represented using a time series of puffs (usually produced at a rate of one per second) with a spatially gaussian mass distribution. The source characteristics are determined by the initial size, mass, temperature, and composition of each puff. The transport and diffusion of each puff is modeled using an empirical gaussian plume methodology developed by Pasquill [11]. In this method, each puff is allowed to travel with the mean atmospheric flow and diffuse

according to empirical laws driven by the atmospheric stability. Puffs are also allowed to rise based on the buoyant force afforded by their temperature. The ACT II model treats the transport of all puffs identically so that the resulting obscurant cloud structure is very smooth and regular; the only cloud structure arises from modeled temporal variations in the obscurant source.

Once a particular obscurant cloud geometry is realized using the transport and diffusion models, the transmission and path radiance may be calculated using a very complete radiative transfer model. The optical properties of the obscurant (extinction coefficient, single scattering albedo, and scattering phase function) must be input by the user. Calculations are performed using only one set of optical parameters; the selection of these parameters determines whether the calculations are valid at a single wavelength, or whether they represent a broadband average result. The scope of the radiative transfer model is illustrated in Figure 2-2. Transmission calculations are performed accounting for aerosol absorption and scattering; as is the case with the LOWTRAN calculations, effects leading to a non-uniform MTF such as multiple scattering are not accounted for. The path radiance calculations are considerably more extensive than those of LOWTRAN. ACT II considers the complete single scattering problem and accounts for:

- Radiation emitted along the path of interest;
- Smoke emissions scattered into the path of interest;
- Plane parallel source emission scattered into the path (eg. solar scattering); and
- Radiation from the sky-ground sphere scattered into the path.

To account for variations in the sky and ground radiation, a sectoring scheme is used. The user may divide the sky into any number of sectors, and supply the diffuse radiance contribution from each sector; the ground is represented by a homogeneous grey body.

An addition to the ACT II radiative transfer model is a very simple path radiance approximation. The purpose of this approximation is to allow very rapid calculations while still including terms indicative of the actual obscurant emission and scattering terms. The radiance equation is:

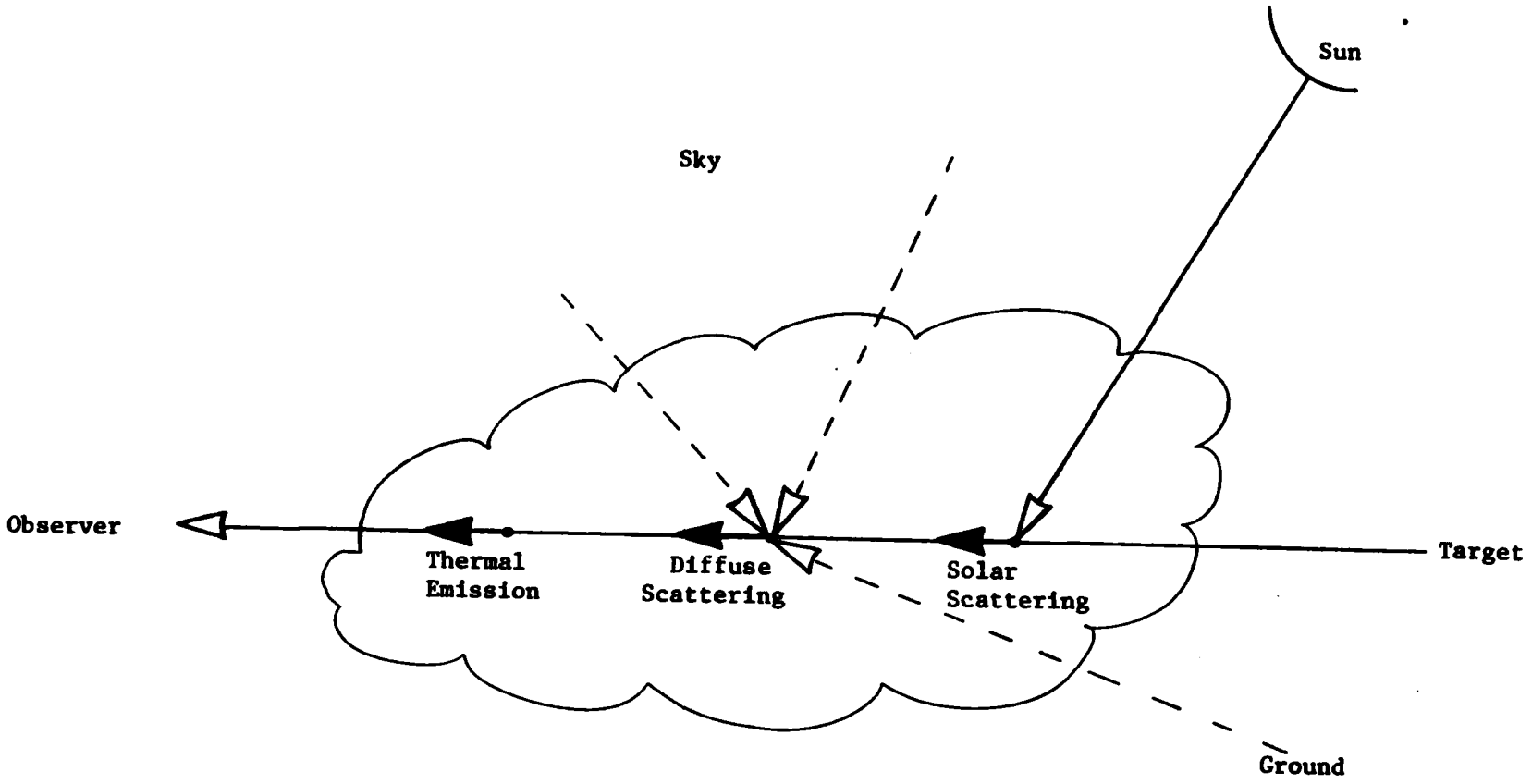

Figure 2-2. Illustration Showing the Effects Considered in the ACT II Radiative Transfer Model

$$L_{p_s}(x\ y) = \left(1.0-\tau_s(x,y)\right)\left[(I_s \bar{P}\ \bar{\omega}) + L_{BB}(T_s)\ (1-\bar{\omega})\right] \quad (2)$$

where $\bar{\omega}$ = Obscurant single scattering albedo

I_s = Total sky/ground irradiance at the obscurant cloud location (W/m^2)

$\bar{P}$ = Scattering phase function weighted by the radiance distribution in the sky and ground hemispheres (Sr^{-1})

T_s = Average obscurant temperature input by the user

L_{BB} = Black body radiance function (W/m^2-Sr)

The approximation is most useful when initially setting up a problem for consideration, and representative results are desired quickly. The full single scattering model should be used when actual simulations are attempted.

2.1.2.2. MADPUFF Transport and Diffusion Methodology

The MADPUFF method is described in several papers and Opti-Metrics reports [2,4,5]. The method is based on work performed by S.R. Hanna [12,13]. The modeling approach assumes that the velocity (u) of a fluid parcel at point (x,y,z) at time t can be represented as the sum of a mean wind component U and a turbulent fluctuation component u':

$$u(x,y,z,t) = U(x,y,z,t) + u'(x,y,z,t) \quad (3)$$

The turbulent fluctuation component u' is also assumed to be the sum of two components such that:

$$u'\ (t + \tau) = u'(t)\ R(\tau) + u'' \quad (4)$$

where $R(\tau)$ = Lagrangian autocorrelation function for time lag τ

= $\exp\ [-\tau/T_L]$, T_L= Lagrangian time scale

u'' = normally distributed random turbulence component with standard deviation given by:

$$\sigma_{u''} = \sigma_u [1 - R^2(\tau)]^{1/2}$$

Hanna combines theory and empirical findings [14] to relate the Lagrangian time scale to more readily observed meteorological quantities:

$$T_{L_{u,v,w}} = 0.17\, z_i/\sigma_{u,v,w} \quad \text{for} \quad \begin{cases} u\text{: } z < z_i \\ v\text{: } z < z_i \\ w\text{: } 100\text{ m} < z < z_i \end{cases} \tag{5}$$

$$T_{L_w} = 0.42\, (z/\sigma_w)\, (u/u^*) \quad \text{for} \quad (w\text{: } z < 100\text{ m})$$

where

z_i = mixing depth

u = mean wind

$\sigma_{u,v,w}$ = Lagrangian standard deviation for u,v,w components, respectively

u^* = friction velocity

z = height above ground

In the MADPUFF method, gaussian smoke puffs are advected by the randomly fluctuating wind vector u; the fluctuating part of the wind (u'') is simulated using a time series of random numbers. Note that although the puffs are advected randomly, their diffusion is still governed by the same empirical relations used in ACT II. However, since the puff diffusion model used in ACT II is intended to represent both the cloud meandering as well as the puff growth, the puff diffusion terms used with MADPUFF are smaller by a factor of 1/3 [11] since the random puff motion is considered separately.

The only remaining difference between the ACT II mode and the MADPUFF mode is the puff buoyancy model. OptiMetrics developed an empirical buoyancy model based on data obtained during the Smoke Week IV and Jefferson Proving Ground trials

[2]; this model is used when the MADPUFF mode is selected. The original ACT II buoyancy model is used when the ACT II mode is selected.

2.2 Sensor Model

Since the sensor model was developed for this simulation, the discussion will of necessity be more detailed than the previous sections. The ISSM sensor model structure was depicted in Figure 2-1. A simple optical system model is used to determine the efficiency with which scene radiation is directed to the system detector(s). The resulting signal map is Fourier transformed so that linear transfer function representations of the sensor subsystems may be easily applied. For convenience, most of the transfer functions incorporated in the model are identical to those used in the NV&EOL Static Performance Model [6]. This means that sensor descriptions used with the NVL&EOL model will also be applicable for use in the simulation. White noise (although any character noise may be accommodated by the model) is inserted following the system detector; the detector is assumed to be the sensor's limiting noise source. After all the transfer functions have been applied, a sensor output image is formed using an inverse Fourier transform. This image may be displayed and evaluated by the user.

2.2.1 Optical System Model

The optical system is characterized in terms of a simple lens defined by its f-number, focal length, and transmission, and a filter defined by its spectral transmission within the sensor bandpass. When combined with the characteristics of a single detector element, the signal from each scene pixel in units of watts is given by:

$$S(x,y) = \frac{\pi A_d}{4\ (f/\#)^2} \int_{\lambda_1}^{\lambda_2} R(\lambda)\ \tau_0(\lambda)\ L_A(x,y)\ d\lambda \qquad (6)$$

where $S(x,y)$ = Detector Signal Map (watts)

A_d = Detector Area (m^2)

$f/\#$ = Optical System F-number

$R(\lambda)$ = Detector Normalized Spectral Response

$\tau_0(\lambda)$ = Optical System Spectral Transmission

$L_A(x,y)$ = Apparent Scene Radiance Map
(w/m^2-Sr-micron)

and in the current version of ISSM, the scene radiance map is assumed to be spectrally uniform.

2.2.2 2-Dimensional Image Fourier Transform

The standard Numerical Analysis Library (NAL) [15] routines SFFT2A and SFFTA are used to perform the Fast Fourier Transform (FFT). Both routines perform the FFT on n-dimensional single precision complex arrays; the difference between the two routines is that SFFT2A requires the number of elements in each array dimension to be a power of two while no such restriction exists for SFFTA.

Before the signal array S can be transformed, the data must be made periodic so that spurious "edge effects" are not introduced. This is done by reflecting the data as illustrated in Figure 2-3. Notice that this procedure does not introduce spurious information into the data; because of the symmetry, all odd Fourier components in both dimensions will be zero. Of course, one may take advantage of this by performing computations using only the non-zero (even) Fourier components.

When performing the Fourier Transform of a 2-dimensional complex array of size nxm, the result is a complex array of the same size. However, when the original array is real, then the transformed array will have conjugate symmetry about each dimension. Thus, all the data information is really contained in a (n/2)x(m/2) complex array; computations need only be performed using one quarter of the transformed array. This means that reflecting the image data (Figure 2-3) has no effect on the number of computations which must be performed in the Fourier domain.

Finally, it should be noted that techniques have been developed to allow real arrays of size n to be transformed using a complex array of size n/2 [16]. Of course, this technique can eliminate the computational penalty involved in taking the Fourier Transform of the reflected image. We have not implemented this approach in the ISSM; however, if very large images (eg. 512x512) are ultimately processed, then consideration of this technique may prove to be important.

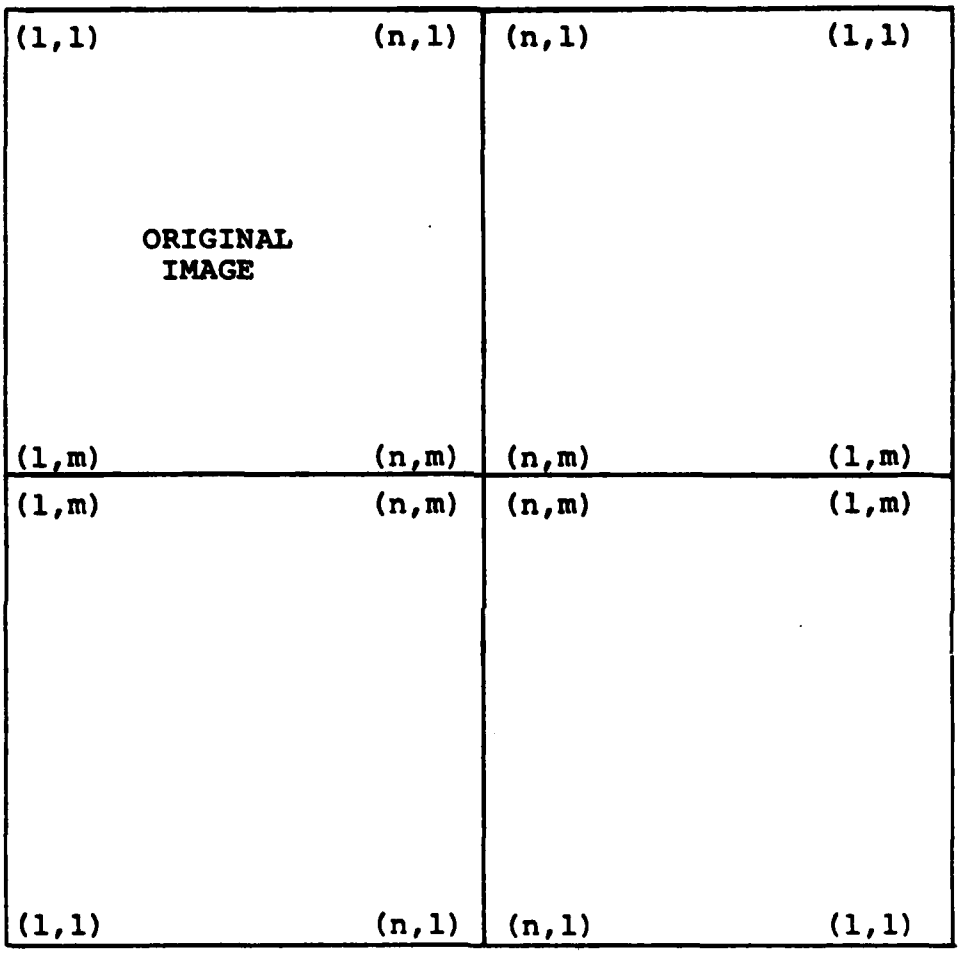

Figure 2-3. Illustration Showing the Image Reflection Scheme used to Eliminate Edge Effects in the Fourier Transform Operation

2.2.3. Sensor Subsystem Transfer Functions

Each sensor subsystem (optics, detector, etc.) is represented by a real or complex transfer function. Because we are operating in the frequency domain, the linear effects of each system element are represented by the product of the transformed image and a transfer function. The complete set of pre-defined subsystem transfer functions is listed in Table 2-1. Not mentioned in the table is the fact that for several subsystems, the user has the option of numerically defining the transfer function. We will briefly comment on each transfer function in the following subsections.

2.2.3.1. Optical System Transfer Functions

Two optical system transfer function forms are provided which describe diffraction by a circular aperture and blur due to optical system aberrations [6]. A gaussian transfer function form is used to represent the blur; it is specified by the 1/e half-width of the corresponding gaussian point spread function. Note that in many real cases, this is not a very realistic representation of optical system aberrations. For these cases, the user may provide a numerical optical system transfer function; transfer functions corresponding to many common aberrations are found in references 17 and 18.

2.2.3.2. Atmospheric Turbulence Transfer Function

The atmospheric turbulence transfer function used in the model originated with Fried [19,20]. We have chosen the near-field formulation of the short exposure case. The near-field assumption encompasses most army scenarios of interest, and the short exposure assumption is consistent with the rapid frame rates of most imaging systems.

Representing the effect of atmospheric turbulence using a Modulation Transfer Function (MTF) is at best a rather crude approximation for several reasons. First, turbulence is dynamic so that it will affect a particular image feature differently at each instant of time. For example, there is a finite probability of obtaining a diffraction-limited view of a particular image feature; the MTF we use is really an average of the degradation caused in an ensemble of short exposure images. The second point is that turbulence effects are not spatially symmetric so that a very specific Complex or Optical Transfer Function (OTF) rather than an MTF is required even at a single instant of time. Indeed, a single MTF description is strictly valid only over a small portion of each image called the isoplanatic patch [21]. However,

Table 2-1. Sensor Subsystem Transfer Function Definitions

Optics - Diffraction

$$H(k_x,k_y) = \frac{2}{\pi}\left[\cos^{-1}(A) - A(1-A^2)^{1/2}\right]$$

$$A = \left(\lambda_D(f/\#)\ k_{xy}\ /F\right)$$

$$k_{xy} = (k_x^2 + k_y^2)^{1/2}$$

λ_D = diffraction wavelength (microns)

f/# = optical system f - number

k_x = spatial frequency in the along-scan dimension ($mrad^{-1}$)

k_y = spatial frequency in the cross-scan dimension ($mrad^{-1}$)

F = optical system focal length (millimeters)

Optics - Blur

$$H(k_x,k_y) = e^{-b(k_x^2+k_y^2)}$$

$b = \pi^2 w^2$

w = e^{-1} half-width of the optical system point spread function (mrad)

Table 2-1. Sensor Subsystem Transfer Function Definitions (continued)

Atmospheric Turbulence

$$H(k_x,k_y) = e^{-3.44\left(\frac{\lambda_D k_{xy}}{1000\ R_0}\right)^{5/3}\left[1.0-0.5\left(\frac{\lambda_D k_{xy}}{1000\ D}\right)^{1/3}\right]}$$

R_0 = atmospheric coherence length (m)

$$= \left[0.159\ C_n^2\left(\frac{2\pi}{1E\text{-}6\ \lambda_D}\right)^2\ r\right]^{-0.6}$$

D = optical system aperture diameter (m)

C_n^2 = refractive index structure parameter ($m^{-2/3}$)

r = sensor-target range (m)

Detector - Temporal Transfer Function

$$H(k_x) = \frac{1.0}{1.0 + j\left(\frac{k_x\ v}{f_D}\right)}$$

$$v = \frac{FOV_x\ FOV_y\ F_r\ \eta_{ov}}{n_p\ IFOV_y\ \eta_{sc}}$$

v = scan velocity (mrad/s)

FOV_x = sensor along-scan field-of-view (mrad)

FOV_y = sensor cross-scan field-of-view (mrad)

F_r = frame rate (s^{-1})

η_{ov} = overscan ratio

n_p = number of detectors in parallel

$IFOV_y$ = sensor instantaneous field-of-view in the cross-scan direction (mrad)

η_{sc} = scan efficiency

Table 2-1. Sensor Subsystem Transfer Function Definitions (continued)

Detector-Spatial Transfer Function

$$H(k_x, k_y) = \text{sinc}(\pi \, IFOV_x k_x) \, \text{sinc}(\pi \, IFOV_y \, k_y)$$

$IFOV_x$ = sensor instantaneous field-of-view in the along-scan direction (mrad)

$\text{sinc}(x)$ = $\sin(x)/x$

Electronics

$$H(k_x) = \left[\frac{1.0}{1.0 + j\left(\frac{k_x v}{f_{LP}}\right)}\right]\left[\frac{j\,\frac{k_x v}{f_{HP}}}{1 + j\left(\frac{k_x v}{f_{HP}}\right)}\right]$$

f_{LP} = electronics cut-off frequency (Hz)

f_{HP} = electronics cut-on frequency (Hz)

Electronic Boost

$$H(k_x) = 1.0 + \frac{(B-1.0)}{2.0}\left[1.0 - \cos\left(\frac{\pi \, v \, k_x}{f_{max}}\right)\right]$$

f_{max} = frequency of maximum boost (Hz)

B = boost at frequency f_{max}

Table 2-1. Sensor Subsystem Transfer Function Definitions (continued)

LEDs

$$H(k_x, k_y) = \text{sinc}(\pi \, LED_x \, k_x) \, \text{sinc}(\pi \, LED_y \, k_y)$$

LED_x = along-scan LED dimension (mrad)

LED_y = cross-scan LED dimension (mrad)

Sampling

$$H(k_x) = \text{sinc}\left(\frac{\pi \, v \, k_x}{2 \, f_{nyq}}\right) e^{-j\left(\frac{\pi \, v \, k_x}{2 \, f_{nyq}}\right)}$$

f_{nyq} = Nyquist frequency determined by the sampling rate (Hz)

Stabilization

$$H(k_x, k_y) = e^{-\left(S_x k_x^2\right)} e^{-\left(S_y k_y^2\right)}$$

S_x = along-scan stabilization parameter ($mrad^2$)

S_y = cross-scan stabilization parameter ($mrad^2$)

if we were to accumulate the specific OTFs which accurately describe the effect of turbulence on short exposure images, we would find the all portions of the image are, on the average, affected in a way described by the MTF listed in Table 2-1.

Finally, a few of the parameters on which the turbulence transfer function depends may be unfamiliar to the reader. The coherence length is the lateral distance over which a wavefront remains coherent after passing through the turbulent media. An interesting interpretation of the coherence length is that the attainable resolution in a long exposure image is approximately equal to that of a diffraction limited system whose aperture diameter is equal to the coherence length. A formula for calculating the coherence length afforded by a homogeneous atmospheric path is listed in Table 2-1. The descriptor of the turbulence strength is the refractive index structure parameter (C_n^2). Reference 22 provides an excellent discussion of turbulence in the atmosphere including the typical diurnal behavior of C_n^2. For convenience, some typical C_n^2 values are listed below:

Time of Day	C_n^2 ($m^{-2/3}$)
sunrise or sunset	1.E-15 or lower
midday	2.E-14 - 6.E-14
midnight	1.E-14 - 2.E-14
extreme midday condition	2.E-13 - 5.E-13

2.2.3.3. Detector Transfer Functions

Two transfer functions have been included to represent the temporal and spatial detector response. The temporal response is modeled by a complex transfer function representing a single pole low-pass filter. The spatial response of the detector is modeled using the 2-dimensional MTF of a rectangular aperture. Of course, this means that the detector elements are assumed to respond uniformly over their entire area.

It should be noted that in this version of the ISSM, we have not considered the effect of cross-scan sampling. In most thermal imaging sensors, cross-scan sampling occurs because the image is scanned in a raster pattern by one or more discrete detectors. Although the effect will be considered along with other non-linear phenomena in later versions of

ISSM, it would be possible to implement an analogous procedure to that used to represent along-scan sampling (section 2.2.3.7) should this be desired by the reader.

2.2.3.4. Electronics Transfer Functions

Two transfer function forms are included to represent the sensor electronics; a complex transfer function representing single pole low-pass and high-pass filters, and a MTF representing a high frequency boost function. The form of the boost function is exactly that used by NV&EOL [6].

2.2.3.5. Light Emitting Diode (LED) Transfer Functions

Virtually all existing thermal imaging systems which incorporate parallel detector arrays use LEDs to either display the image directly, or as part of an Electro-Optic (EO) multiplexer. The LEDs are assumed to be rectangular; their spatial transfer function is identical in form to that of the sensor detectors. No temporal filtering by the LEDs in the along-scan dimension is considered, and any sampling effects which involve the LEDs are ignored.

2.2.3.6. Vidicon Transfer Function

No default transfer function form is included for a vidicon; the user must input a numerical definition. The vidicon (which is the video multiplexer in most current technology infrared imaging systems) is really a complete EO system in its own right. Typically, it will have an asymmetric transfer function that may include boost in the along-scan dimension. Thus, it is difficult to provide a suitable default transfer function form.

2.2.3.7. Digital Multiplexer (Sampling) Transfer Function

In a digital multiplexer system, the LEDs and vidicon which make up the EO multiplexer are replaced by an electronic circuit which combines the output of each detector in a single video stream. In a typical electronic multiplexer, each detector signal is applied to a separate charge accumulator, and its signal is integrated for one sample period. The accumulated charges are then gated to a serial charge transport register. By reading the entire contents of this register within one sample period, a serial video stream is formed. Note that the video is serial in the cross-scan dimension; thus the process introduces sampling in the along-scan direction.

The transfer function given in Table 2-1 accounts for both the integration and sampling of the assumed electronic multiplexer. The sinc function arises from assuming that the charge accumulator is represented by an ideal or "box-car" integrator. Finally, the Nyquist frequency is simply one half the sampling rate; the transfer function is written assuming that the sample period and integration period are exactly matched.

2.2.3.8. Stabilization Transfer Function

The stabilization transfer function may be defined either numerically, or using the default gaussian form. The input parameters for the gaussian form are exactly the same as those used in the NV&EOL model [6]. Note that the parameters S_x and S_y may be related to the stabilization-limited point spread function 1/e halfwidth as indicated in the optical system blur transfer function formula.

2.2.4 Detector Noise Model and Implementation

The ISSM allows noise to be added at a point just following the system detector(s). The technique used is to compute a random sample of noise and then add this sample to the scene signal in the frequency domain. All sensor subsystems following this point of noise insertion then act on both the signal and noise. Adding the noise in the frequency domain is very convenient in that it is trivial to account for any arbitrary noise power spectrum, and additional Fourier Transform operations are avoided. However, to avoid confusion, it should be noted that the current ISSM configuration uses a simple white noise model.

Use of a white noise model is justified in many cases of interest. For example, photovoltaic or photoconductive detectors are well represented by a white noise spectrum over a broad range of intermediate frequencies limited only by the detector temporal response at very high frequencies, and 1/f noise at very low frequencies. In practical imaging sensor applications, the system electronics usually restrict the system bandwidth well below the detector high frequency response. Further, the 1/f noise is usually filtered by ac coupling between the detectors and their preamplifiers.

The modeled noise power spectral density is given as follows:

$$\Phi_n(f) = \frac{A_d}{n_s(F_r\ T_e)\ (D^*)^2} \tag{7}$$

where

Φ_n = noise power spectral density (W^2/Hz)

A_d = detector element area (cm^2)

n_s = number of detectors in series

F_r = frame rate (s^{-1})

T_e = eye integration time (s)

D^* = detector peak detectivity ($cm-(Hz)^{1/2}/w$)

There are several points concerning this expression which deserve comment. First, it should be emphasized that the detector D^* characteristic is spectrally dependent. It is important that the noise be calculated using the D^* relevant at the point of peak spectral response (as defined by the response characteristic $R(\lambda)$ in equation 6) in order to be consistent with the way that the signal is defined. Second, the quantity n_s is present to account for Time Delay and Integration (TDI) techniques which can be used to reduce noise in sensors which have multiple detectors positioned in series. Finally, the term $(F_r T_e)$ attempts to correct for the fact that the simulation can only compute a single, static image for display to an observer. In a real sensor, a number of image frames with statistically independent noise samples may be presented to the observer within one eye integration time. Because of this, the observer using the real sensor can obtain a better image signal-to-noise ratio than can be obtained with the static image. Of course, the approximate correction for this is the term given above.

The actual sample of noise which is added to an image pixel in the Fourier doman is computed as follows:

$$\text{Noise}_i = \left(\frac{\Phi_n}{2}\right)^{1/2} N_k + j \left(\frac{\Phi_n}{2}\right)^{1/2} N_{k+1} \qquad (8)$$

where Noise_i = noise added at a point in the fourier domain ($W/(H_z)^{1/2}$)

N_k = normally distributed random number with zero mean and unit variance

We are simply computing a field of normally distributed complex random numbers whose mean is zero and whose variance is the white noise power spectral density. Note that it would be a trivial matter to include a non-white power spectrum in equation 8 should that become necessary in the future.

3.0. User's Guide

The routines which comprise the Imaging Sensor Simulation Model (ISSM) may be grouped into six general categories:

1. control routines,
2. frame I/O interface routines,
3. sensor module routines,
4. atmospheric effects module routines,
5. battlefield effects module routines, and
6. image display routines.

Tables 3-1 through 3-6 provide descriptions of each subprogram included in each of these six categories.

3.1. Using the Simulation

3.1.1. Logical Unit Assignments

A large number of auxiliary input/output unit assignments are necessary to use all the features of the simulation. For example, data libraries may be used to input complicated sets of input parameters such as those required by the sensor module and the battlefield effects module. Similarly, the image output may take a number of forms such as video display, printer plots, and formatted or unformatted files on tape.

Table 3-7 presents a list of the input/output units currently used in the simulation. A brief description of the unit's purpose and the form of the input or output is provided.

3.1.2. Menu Hierarchy

The simulation is structured around a menu tree which allows the user to access the various modules in any logical order. Each menu returns control to the menu from which it was called after it either performs its functions or is explicitly told to return by the user. Since menus may be nested several levels deep, it is important for the user to become familiar with the menu hierarchy. Figures 3-1 through 3-5 provide a schematic representation of the menu hierarchy in the simulation which will enable the user to visualize how one can pass through the menus to access certain features of the model. Figure 3-1 provides the main menu structure and the menus immediately accessed from it. Figures 3-2 through 3-5 detail the menu structure of the four major modules: the frame I/O interface, sensor, atmospheric effects, and battlefield effects modules.

Table 3-1. Control Routines Included in Simulation

These routines set up the initial conditions and provide an interface between the main menu and individual modules.

Routine	Description
MAIN	Reads in sensor library, sets terminal type, selects main menu options.
BLOCK DATA	Default values for variables input by menus.
LIBR	Interface with frame I/O routines.
SNSR	Interface with sensor routines.
ATMOS	Interface with atmospheric effects module.
BATTLE	Interface with battlefield effects module.
PRLINE	Interface with image display routines.

Table 3-2. Routines Included in Frame I/O Interface

Routine	Description
LIBR	Selects options for input or output to a data library.
FRREAD	Reads frame from file and/or selects a part of frame for processing.
TAPEO	Outputs frame to a library.

Table 3-3. Routines Included in Sensor Effects Module

Routine	Description
SNSR	Displays sensor menu, calls routines for appropriate options.
SENCHR	Modifies sensor characteristics according to user inputs.
TFSWCH	Selects which transfer functions will be applied to represent sensor effects.
TRNSFM	Calls Fourier transform routines, optical transfer function routine.
OTFS	Sets up and calls optical transfer functions.
HODIF	Diffraction optical transfer function.
HBLUR	Blur optical transfer function.
HTURB	Atmospheric turbulence transfer function.
HDET1	Spatial detector transfer function.
ZDET2	Temporal detector transfer function.
ZELEC	Electronics transfer function.
HBOOST	Electronic boost transfer function.
ZSAMP	Along-scan sampling transfer function.
SRESP	Calculates optical system response.
SFFTA	Fast Fourier transform for an arbitrarily dimensioned array.
SFFT2A	Fast Fourier transform for an array whose dimensions are powers of 2.
ALINEY	Linear interpolation routine.
QTFE	Integration routine.

Table 3-4. Routines Included in Atmospheric Effects Module

Routine	Description
LWTRN6	Calls subroutines to compute transmittance and radiance.
NSMDL	For user-defined atmospheric or aerosol profiles.
SUBSOL	Calculates the subsolar point angles based upon time and day.
STDMDL	Sets up atmospheric profiles of attenuator densities.
AERPRF	Computes scaling factor profiles for aerosols.
GEO	Driver for air mass subroutines. Calculates attenuator amounts for the slant path.
SSGEO	Obtains attenuator amounts from scattering points along optical path to the extraterrestrial source.
EXABIN	Loads aerosol extinction and absorption coefficients for the appropriate model and relative humidity.
TRANS	Calculates transmittance, atmospheric radiance, and solar/lunar scattered radiance for slant path.

Table 3-4. Routines Included in Atmospheric Effects Module (continued)

Routine	Description
GEO	Driver for air mass subroutines. Calculates attenuator amounts for the slant path.
GEOINP	Interprets geometry input parameters into the standard form H1, H2, ANGLE, and LEN.
FNDHMN	Calculates HMIN, the minimum altitude along the path and PHI, the zenith angle at H2.
REDUCE	Eliminates slant path segments that extend beyond the highest profile altitude.
FDBETA	Calculates angle, given H1, H2, and BETA by iteration.
RFPATH	Determines the refracted path and the absorber amounts through all the layers.
FILL	Defines the boundaries of the slant path and interpolates densities at these boundaries.
LAYER	Calculates the path and amounts through one layer.
RADREF	Computes radius of curvature of the refracted ray for a horizontal path.
FINDSH	Finds layer boundaries and scale height at ground for index of refraction.
SCALHT	Calculates scale height of index of refraction.
ANDEX	Computes index of refraction at a specific height.
EXPINT	Performs exponential interpolations for the geometry routines.

Table 3-4. Routines Included in Atmospheric Effects Module (continued)

Routine	Description
SSGEO	Obtains attenuator amounts from scattering points along optical path to the extraterrestrial source.
PSIDEL	Calculates the relative azimuth between the line of sight and the direct solar/lunar path.
PSI	Returns solar azimuth relative to line-of-sight at current scattering location.
DEL	Returns solar zenith angle at any point along optical path.
GEO	Driver for air mass subroutines. Calculates attenuator amounts for the slant path.
SCTANG	Returns the scattering angle at any point along the optical path.
TRANS	Calculates transmittance, atmospheric radiance, and solar/lunar scattered radiance for slant path.
AEREXT	Interpolates aerosol attenuation coefficients to required wavenumber.
HNO3	Determines nitric acid absorption coefficient at required wavenumber.
TRANFN	Calculates transmittance for ozone, uniformly-mixed gases, and water vapor.
SOURCE	Contains solar intensity data and calculates lunar intensity.
TNRAIN	Calculates transmittance of rain as a function of rain rate and slant range.
SSRAD	Performs the layer by layer single scattering radiance sum.

Table 3-4. Routines Included in Atmospheric Effects Module (continued)

Routine	Description
PHASEF	Chooses correct phase function based on relative humidity, frequency, scattering angle, and model.
INTERP	Performs linear or logarithmic interpolation.
PF	Returns the appropriate phase function from the stored database.
C1DTA	Returns water vapor band absorption coefficient at required wavenumber.
C2DTA	Returns uniformly-mixed gases absorption coefficient at required wavenumber.
C3DTA	Returns ozone band absorption coefficient at required wavenumber.
C4DTA	Returns N_2 continuum absorption coefficient at required wavenumber.
C6DTA	Returns molecular scattering attenuation coefficient at required wavenumber.
C8DTA	Returns ozone UV and visible absorption coefficient at required wavenumber.
SLF296	Loads self-broadened water vapor continuum at 296°K.
SLF260	Loads self-broadened water vapor continuum at 260°K.

Table 3-4. Routines Included in Atmospheric Effects Module (continued)

Routine	Description
FRN296	Loads foreign-broadened water vapor continuum at 296°K.
SINT	Performs interpolation for vapor continuum.
MDTA	Model atmospheric data.
PRFDTA	Aerosol profile data.
EXTDTA	Aerosol extinction and absorption data.
SF296	Self-broadened absorption coefficients for water vapor continuum at 296°K.
SF260	Self-broadened absorption coefficients for water vapor continuum at 260°K.
BFH20	Foreign-broadened absorption coefficients for water vapor continuum at 296°K.
TRFN	LOWTRAN transmittance functions.
C1D	Water vapor band model absorption coefficients.
C2D	Uniformly-mixed gases band model absorption coefficients.
C3D	Ozone band model absorption coefficients.
C4D	Nitrogen continuum absorption coefficients and UV ozone absorption coefficients.
PHSDTA	70 averaged phase functions and truth table identifying correct phase function.

Table 3-5. Routines Included in Battlefield Effects Module

Routine	Description
BATTLE	Sets up geometry, provides control over options.
AMGREN	Calls routines for performing calculations.
DATRD	Reads input deck from library.
SCLOS	Calculates vectors for calculation matrix.
BNORM	Normalizes munition burn rate function coefficients.
MADPR	Calculates parameters for use by MADPUF.
UWIND	Calculates average wind speed at a given height.
RANDOM	Generates normally distributed random numbers.
TEMP	Calculates temperature at a given height.
BURN	Calculates burn function at a given time.
MADPUF	Computes transport and diffusion of random puffs.
PUFTEM	Calculates puff centroid temperatures.
BUOY	Computes buoyant rise.
YIELD	Calculates yield factor and acid mass fraction for phosphorus smoke.

Table 3-5. Routines Included in Battlefield Effects Module (continued)

Routine	Description
BRISE	Prepares plume rise parameters for exponential rise model.
TRNDF	ACT II transport and diffusion model.
CLDHT	Computes cloud temperature and buoyant rise in ACT II model.
ERFUN	Computes error function by numerical approximation.
SCTCO	Computes cosine of angle between two vectors.
BBRAD	Evaluates blackbody function.
SATPR	Computes water vapor partial pressure.
CLDRD	Performs cloud radiance calculations.
PATHR	Computes radiance over a path segment.
SECTR	Computes sky sector radiance.
PHASE	Calculates phase function at a specific angle.

Table 3-6. Routines Included in Image Display Module

Routine	Description
PRLINE	Selects output choice, performs line printer variable density plots.
FIND	Determines minimum and maximum values in array.
COMTAL	Writes binary array to a file, pads with zeros, for reading by COMTAL.
TAPE	Writes image array to a formatted file.

Table 3-7. I/O Units Used in the Simulation

Unit #	Input (I) Output (O)	Description	Form of I/O
0*	I	Battlefield effects module input	80 column card images
3	O	Printer plot output for producing variable density printer plots	ASCII characters 20_{16} 44_{16} for 37 gray levels
5	I	Interactive (terminal) inputs	List directed
6	O	Interactive (terminal) outputs (menus, prompts)	Formatted
7	O	Screen clear characters to terminal	Unformatted
8	I/O	Sensor parameter library	Fixed-length 1233 character records
9	O	COMTAL display file	256x256 byte data array
11	O	Formatted frame output	E10.3 format
15*	I	Scene radiance map	80 character header. Each data record read 512A4 format

* Unit number may be changed within the program.

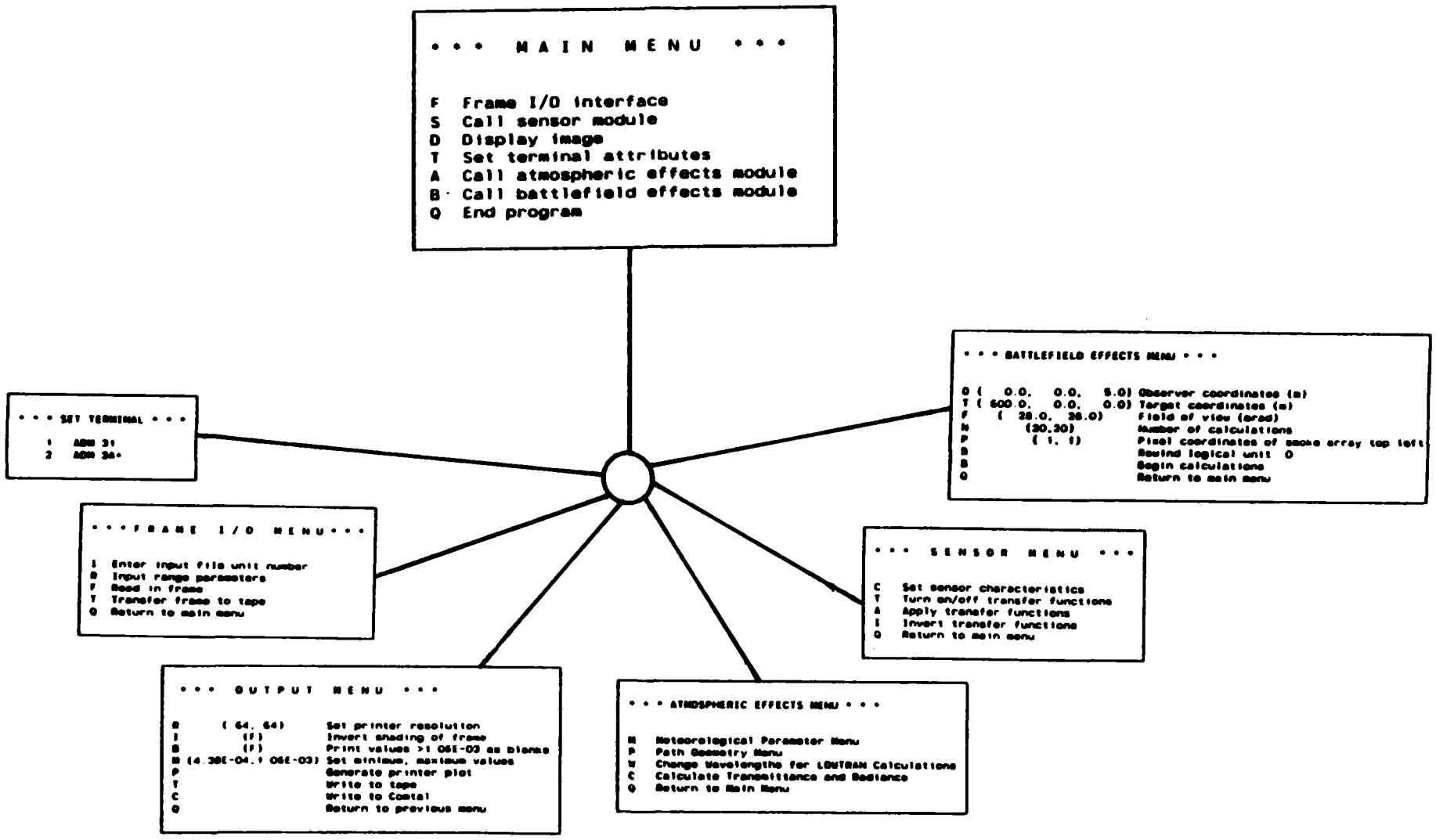

Figure 3-1. Main Menu and Menus Called by Main Menu

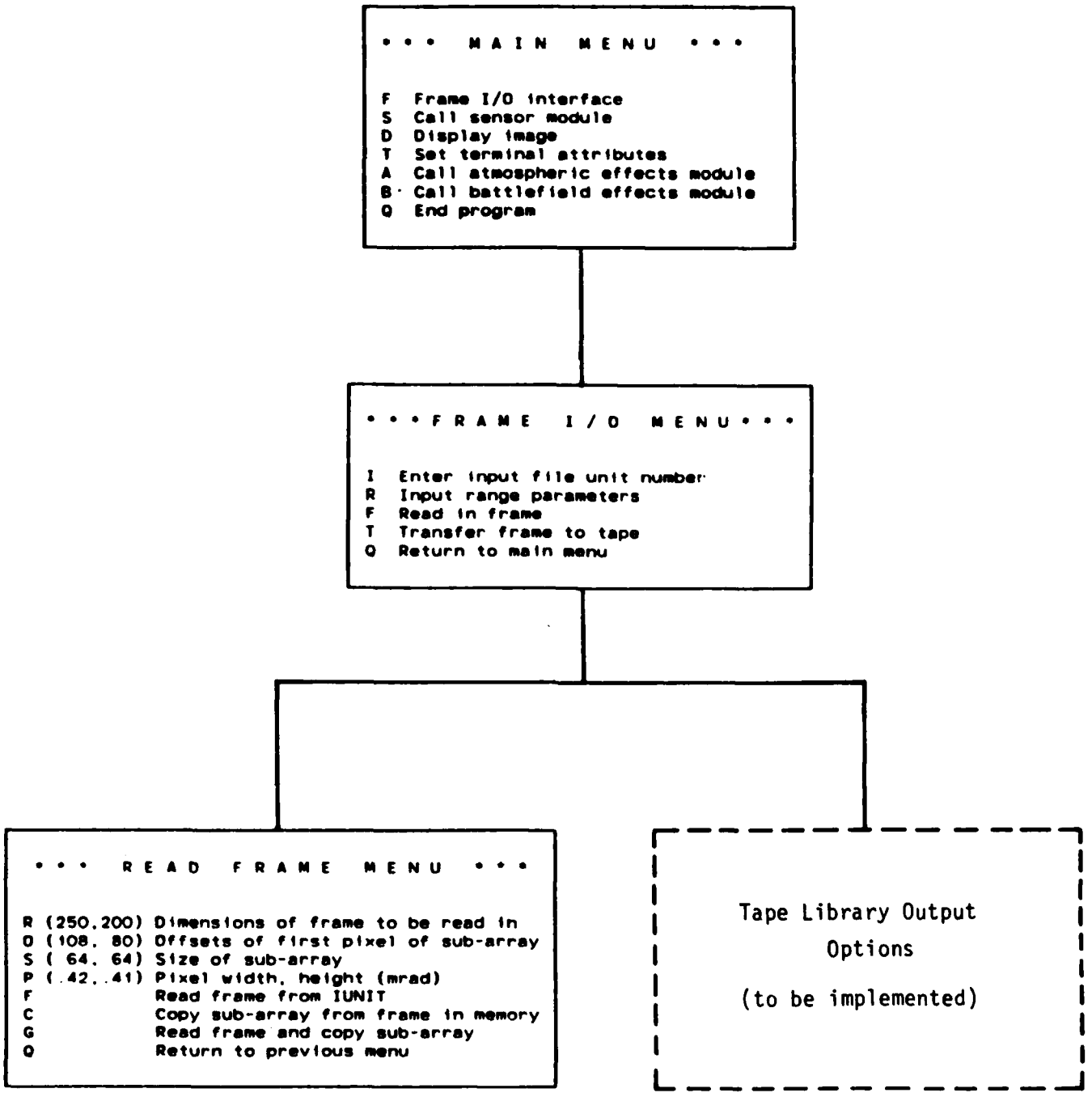

Figure 3-2. Menu Structure of Frame I/O Interface

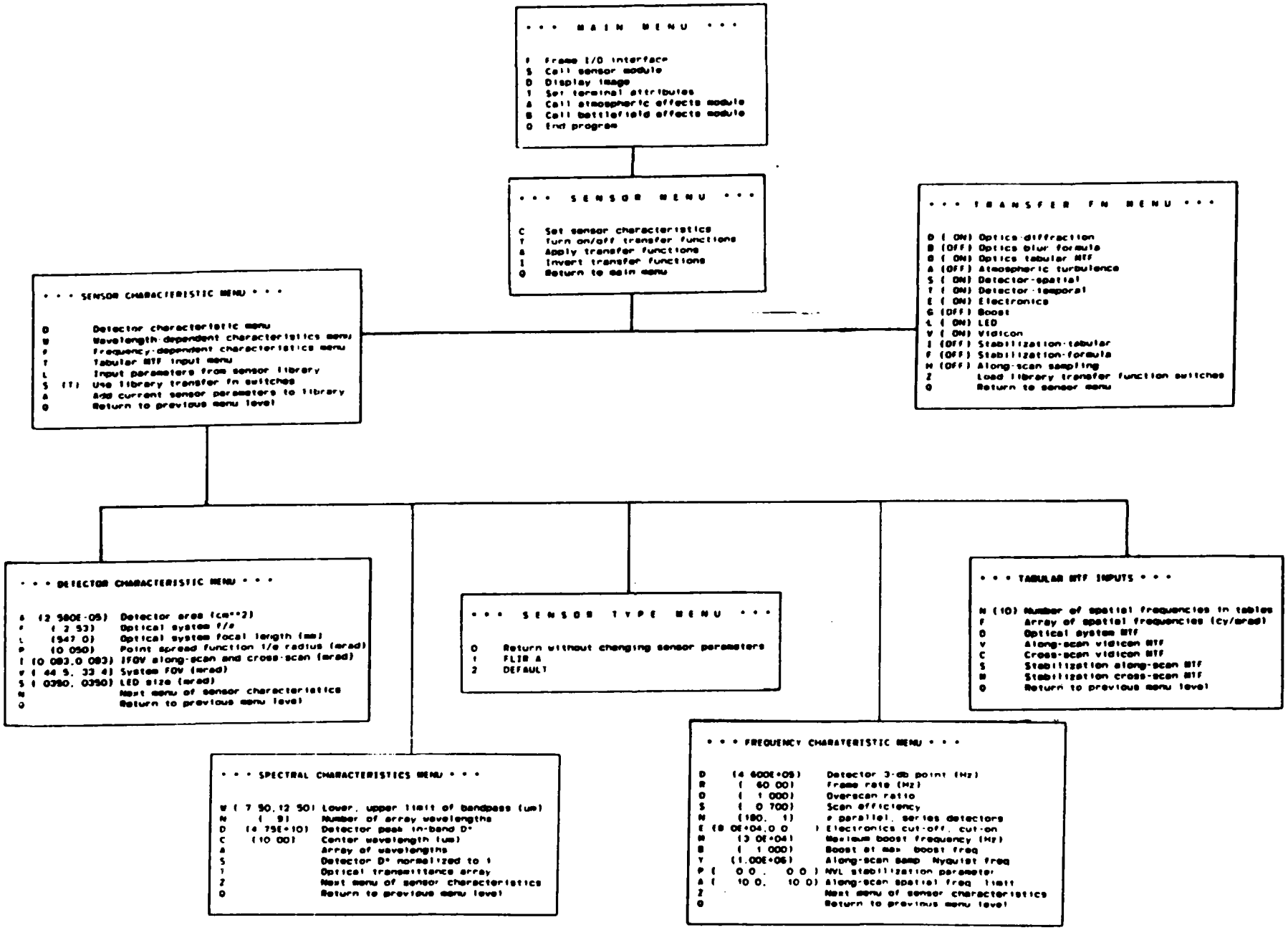

Figure 3-3. Menu Structure of Sensor Module

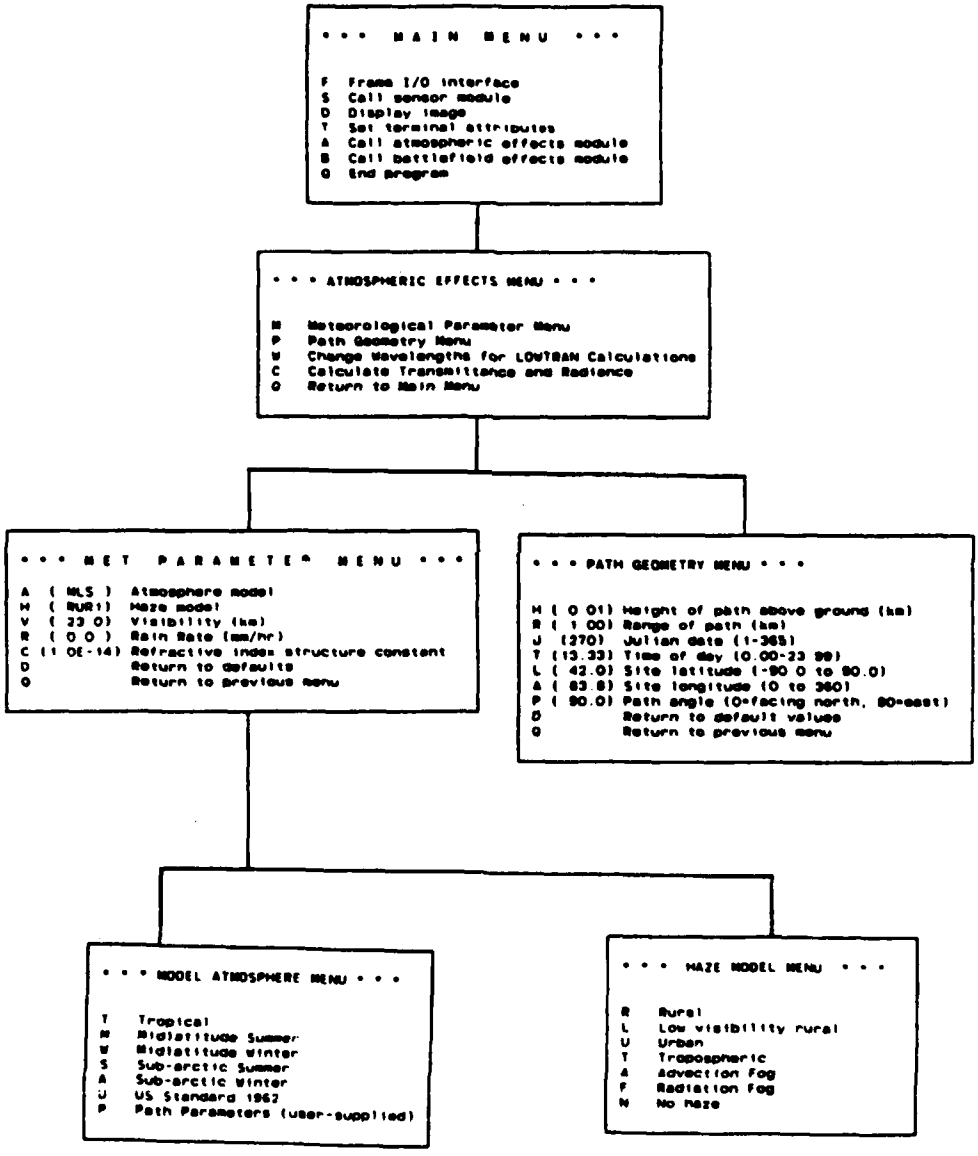

Figure 3-4. Menu Structure of Atmospheric Effects Module

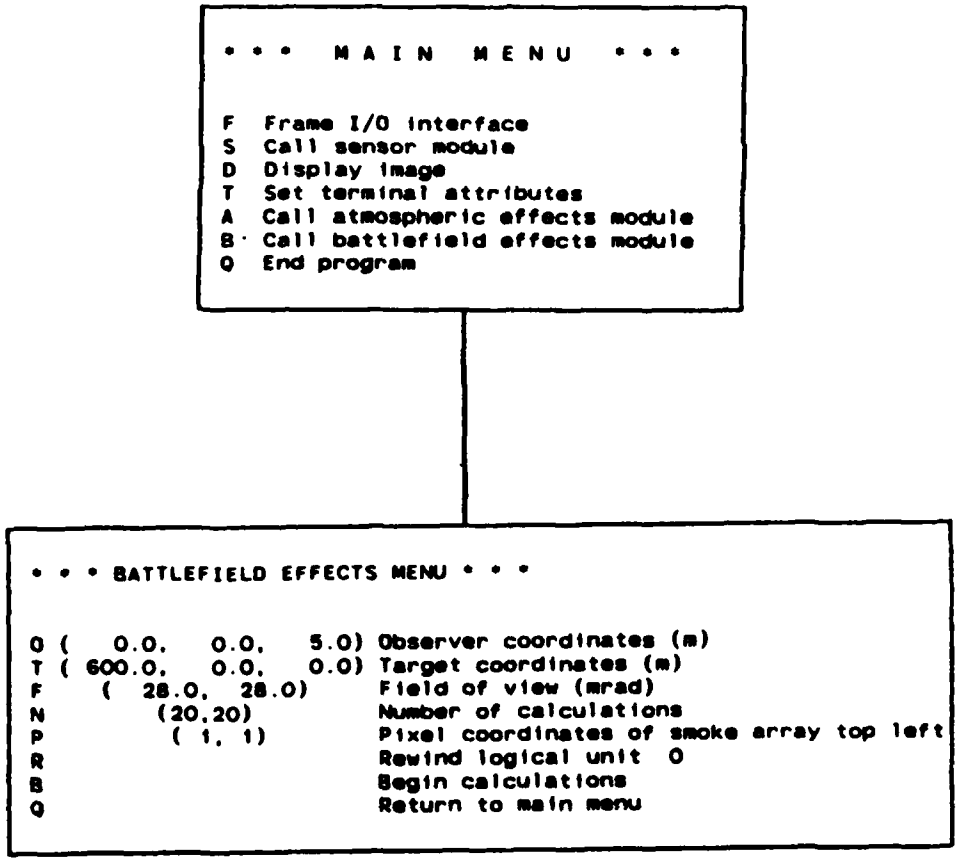

Figure 3-5. Battlefield Effects Module Menus

Most menus which allow the input of values for particular variables display the current values for the variables in the menu itself. After a new value is input, the menu is then immediately updated to allow the user to verify that the value was read in correctly. All numeric values are read using list-directed format, which eliminates the necessity of entering the values in a particular format. The menus themselves accept single ASCII character inputs. Only the first character entered is examined, and if a character is entered which does not correspond to a menu choice, the menu is displayed again to allow the user to make an appropriate choice.

Each menu display is preceded by a screen clear character. Since individual terminals require different ASCII characters to clear the screen, the main menu allows the user to select the appropriate screen clear character by choosing from a library of terminal types. Currently, only screen clear commands for the ADM 31 and ADM 3A+ terminals are provided. Appropriate values for the DEC terminals used at TACOM will be added to the library.

3.1.3. Order of Execution

The order of execution of the routines in the simulation may be varied to allow the user maximum flexibility. However, some care should be taken to insure that the individual modules are executed in a logical order. For example, it would be incorrect to apply the sensor transfer functions before running the atmospheric effects module to attenuate a zero-range radiance map. This section will discuss the order in which the modules should be executed for several typical uses of the simulation.

The simplest use of the simulation involves reading in a scene radiance map and displaying some portion of it. To accomplish this, the user should proceed as follows:

1. Call frame I/O interface routines.

2. Select option to read in a frame.

3. Input necessary parameters for dimensions of the frame to be read in and subset of the frame of interest.

4. Read in the frame and copy a subset of the frame to the image array.

5. Return to main menu.

6. Select display image option.

7. Display unprocessed image in the desired manner.

To display a scene radiance map attenuated by atmospheric effects, the process is only slightly more complicated:

1. Follow steps 1-5 above.

2. Call atmospheric effects module.

3. Input appropriate meteorological parameters, path geometry parameters, and the wavelengths at which calculations are to be performed.

4. Calculate transmittance and radiance.

5. Display image (steps 6-7 above).

Instead of attenuating the scene radiance map with a natural atmosphere, attenuation by a battlefield environment may be modeled. The procedure is similar to the previous case, except that instead of step 4 above, the user should return to the main menu after entering the atmospheric effects module parameters and call the battlefield effects module. The user then sets up the inputs for the battlefield effects module and performs the calculations.

The effects of a sensor should always be introduced after the atmospheric effects module and/or battlefield effects module have been executed. The appropriate order of execution is:

1. Read in frame.

2. Call atmospheric effects module and/or battlefield effects module.

3. Call sensor module

   - input sensor characteristics or read in sensor parameters from a library

   - select transfer functions to be applied

   - apply transfer functions.

4. Display image.

Notice that once a scene radiance map has been read in, the user may process the map in several different ways without having to re-read the entire map. This is accomplished through use of the "copy sub-array" option in the frame I/O interface routines. The original scene radiance map is always available in memory and is not modified by execution of the various modules. The user may repeatedly return and copy some subset of the radiance map into the image array for processing.

The user may at any time display the existing image array. In a given run, the user may display the original radiance map, the radiance map attenuated by atmosphere, the radiance map after applying the battlefield effects module, and the image after applying the sensor transfer functions.

A sample terminal session is provided in appendix B which will help the user to become familiar with the order of execution. The session produces five sample images which include application of the atmospheric effects module, battlefield effects module, and sensor module.

3.1.4. Scene Geometry

Scene geometry is specified by the field of view per pixel of the scene radiance map, the angular dimensions of the scene radiance map, and the range of the scene radiance map from the sensor. For running the sensor module and the atmospheric effects module, no additional geometry information is required. For running the battlefield effects module, the geometry is more complex and additional input parameters are required.

It is important to note that when running the model to simulate a sensor at a range other than the range at which the actual data were taken, the field of view per pixel must be appropriately adjusted. Figure 3-6 demonstrates the geometry. The appropriate relationship between field of view per pixel and range is:

$$F_x(r_s) = (r_m/r_s)\, F_x(r_m)$$
$$F_y(r_s) = (r_m/r_s)\, F_y(r_m) \qquad (9)$$

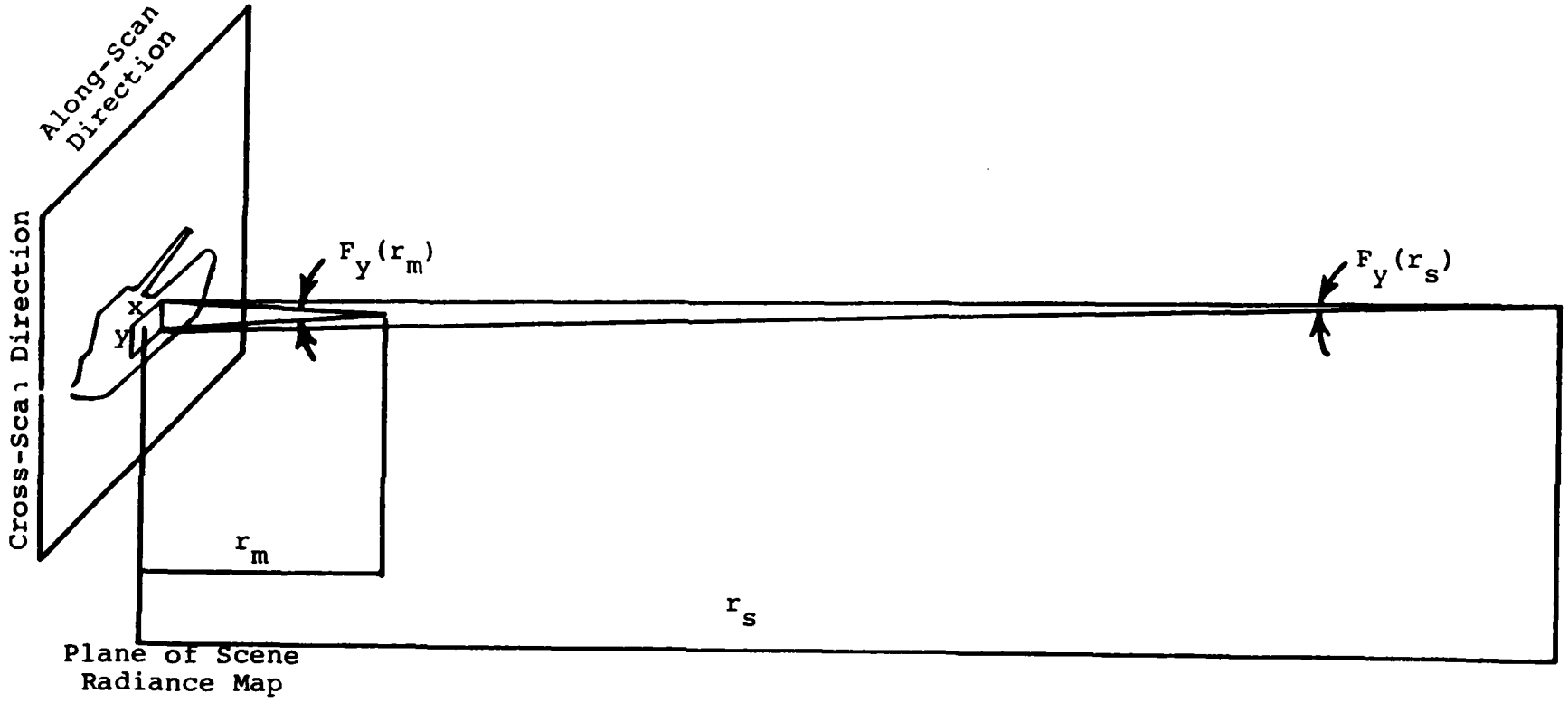

Figure 3-6. Relationship between Field of View per Pixel (F_x,F_y) and Range when Simulating a Sensor at a Distance r_s. The Scene Radiance Map was Obtained from a Sensor at Distance r_m with a Cross-Scan Field of View per Pixel $F_y(r_m)$.

where: $F_x(r)$, $F_y(r)$ = Field of view per pixel at range r from the radiance map (along-scan, cross-scan)

r_s = Range of sensor from radiance map in the simulation

r_m = Range of sensor from radiance map when the actual data was taken.

For the battlefield effects module, the particular scenario of smoke munition locations and meteorological conditions must be read in from a library. Geometry inputs which must be set up in this library include the coordinates of the sources and a reference angle, PHNOR, which specifies the heading of north clockwise from the Y-axis. The value of PHNOR is used in the model only for the purpose of relating wind direction to the coordinate system.

The values needed to define the observer-target lines of sight are input by the observer in the battlefield effects module. A grid of lines of sight dimensioned up to 20x20 is specified, with the dimensions of the grid and field of view of the grid defined by the user. This grid is known as the smoke grid. The coordinates of the observer and the end of the lower left line of sight in the grid must be specified using the coordinate system defined in the input card deck. This geometry is represented in Figure 3-7. There must also be a way of specifying the relationship between the smoke grid and the scene radiance map array. To do this, the user must provide the pixel coordinates of the top left corner of the smoke grid. Figure 3-8 describes the relationship between the lines of sight in the smoke grid and the pixels in the image array. Note that negative values may be given for the pixel coordinates of the smoke grid, although this is wasteful of computer resources since it means calculations must be performed to obtain transmittances and radiance values for lines of sight which are outside the image bounds.

In order to obtain the desired scene geometry, the user is advised to prepare a scenario with the smoke sources near the origin of a convenient coordinate system. A qualitative drawing of the smoke source locations, wind direction, and the resulting smoke cloud should be shown in a figure similar to Figure 3-7. Then, the observer location and smoke grid points can be defined in terms of this coordinate system. To relate the smoke grid to the image array, the user should display the scene radiance map on the COMTAL image

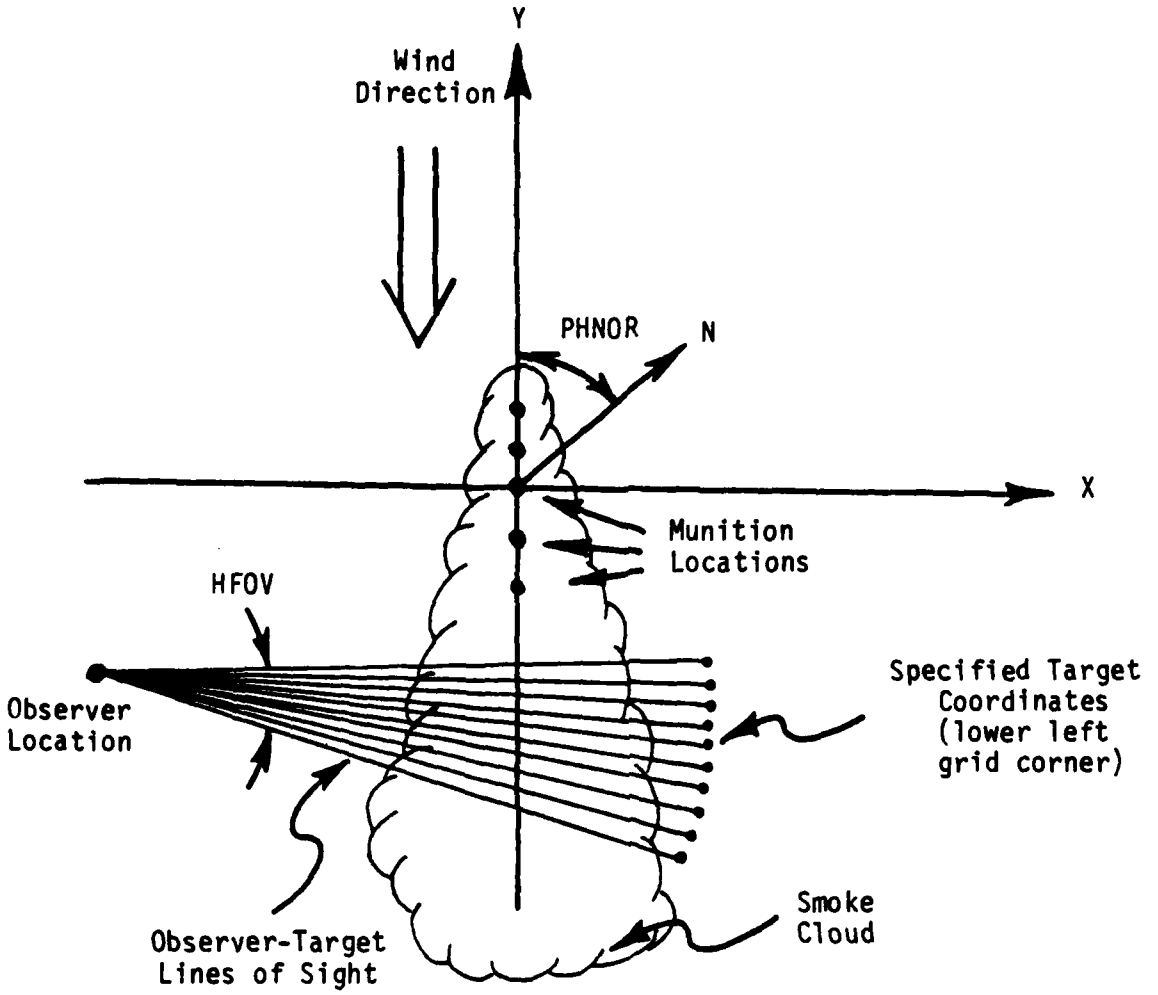

Figure 3-7. Sample Geometry Inputs for a Typical Smoke Scenario. Munition Locations, Wind Direction, and PHNOR are Specified in Smoke Scenario Input Deck. Observer Location, Specified Target Coordinates, Dimensions of Observer-Target Line of Sight Grid, and Field of View of Line of Sight Grid are Input via Battlefield Effects Menu. In this case, PHNOR = 40°, Wind Direction = 320°.

processor before entering the battlefield effects module. By noting the location of the objects of interest in the image and recalling the horizontal and vertical fields of view of the image, the smoke grid may be appropriately positioned.

Despite the best efforts of the user, more than one attempt may be necessary to obtain the desired geometry. The simulation allows the user to rewind the smoke input data file, re-copy the undistorted image from the frame in memory, and repeat the battlefield effects module calculations using different parameters without the need to terminate the program.

3.1.5 Run-Time Performance of the Simulation

The current version of the simulation requires one megabyte of virtual memory ($FF600_{16}$ bytes). This is with the image array and the scene radiance map each dimensioned to 256 x 256. No attempt has been made to reduce memory requirements by operating the simulation in an overlaid mode. This will not save much memory, however, because more than 75% of the memory in use is required for the scene radiance map and image array.

Current CPU time requirements on the VAX 11/750 are a strong function of the paging demands on the system. As a result, time requirements do not increase linearly with the number of arithmetic operations required. On the University of Michigan's Amdahl 5860 system, paging operations are considerably faster and CPU requirements vary nearly linearly with the number of operations.

Two test cases were run to demonstrate the CPU time requirements of the simulation. The conditions corresponded to those listed in Table 3-8. Run time and CPU time required to execute each of the major routines are listed in Table 3-9 for operation on both the VAX 11/750 and Amdahl 5860 systems.

Of particular interest in the time comparisons is the dramatic increase in CPU time and real time which results when the array dimensions are doubled and the sensor transfer functions applied on the VAX system. Although the number of computations increases by only a factor slightly greater than four, CPU time requirements increase by a factor of 13 and real time requirements increase by a factor of nearly 25. These cases were run with the process limits described in Table 3-10. A total of 321,587 page faults occurred when the transfer functions were applied to the 128 x 128 array

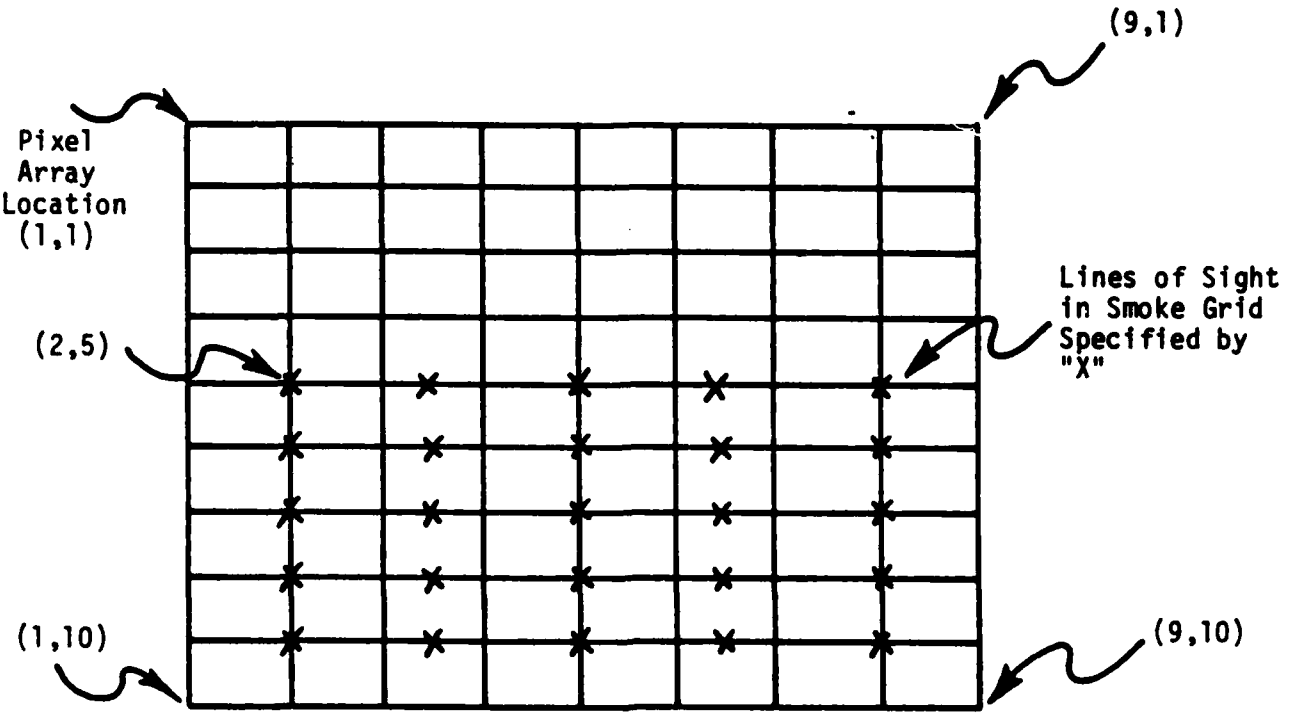

Figure 3-8. Relationship between Pixel Array and Grid Specified in Battlefield Effects Module. For this case, a 9 x 10 Pixel Array and a 5 x 5 Smoke Grid are used. The Top Left Line of Sight in the Smoke Grid Corresponds to Pixel Array Element (2,5). The Vertical Field of View per Grid Point is Equal to the Vertical Field of View per Pixel; the Horizontal Field of View per Grid Point is Equal to 1.5 Times the Horizontal Field of View per Pixel. Calculations of Obscuration at each Pixel Array Location are Based on Two Dimensional Interpolation within the Smoke Grid.

Table 3-8. Scenarios Used in Timing Tests

SCENARIO 1

Array Size: 64x64*

Sensor transfer functions used: default

Atmospheric Effects Module conditions:

Midlatitude summer model atmosphere
Rural haze model
23 km meteorological range
0.0 mm/hr. rain
800-1240 cm^{-1} in 20 cm^{-1} steps

Battlefield Effects Module conditions: none

SCENARIO 2

Array size: 128x128**

Sensor transfer functions used: default

Atmospheric Effects Module conditions:

Midlatitude winter model atmosphere
Advection fog
1 km meteorological range
1.0 mm/hr. rain
800-1250 cm^{-1} in 5 cm^{-1} steps

Battlefield Effects Module conditions:

4 L8A1 grenades
5 sec. after burst
Random puff mode

* Fourier transforms are performed on a 128x128 complex array to avoid edge effects.

** Fourier transforms are performed on a 256x256 complex array to avoid edge effects.

Table 3-9. Results of Timing Tests. Scenarios correspond to those described in Table 3-8

	Time Required (sec)			
	VAX 11/750		Amdahl 5860	
SCENARIO 1	Real	CPU	Real	CPU
Initial Overhead	2	1.90	8	0.276
Read Frame	12	11.17	5	0.596
Sensor Transfer Functions	28	25.52	4	1.068
Atmospheric Effects Module	4	1.87	1	0.105
SCENARIO 2				
Initial Overhead	2	1.90	8	0.276
Read Frame	13	12.49	5	0.646
Sensor Transfer Functions	695	335.76	13	4.491
Atmospheric Effects Module	6	4.57	2	0.302
Battlefield Effects Module	60	44.36	18	2.423

Table 3-10. Process Limits on the VAX 11/750 under which the Test Cases were run

Priority	4
Buffered I/O byte count quota:	4096
Timer queue entry quota:	10
Paging file quota:	9851
Default page fault cluster:	64
Enqueue quota:	20
Working set quota:	500

as compared with only 179 for the 64 x 64 array. Each Fourier Transform required only five seconds of real time for a 128 x 128 complex array, as compared to an average of 285 seconds for a 256 x 256 complex array.

3.2. Sensor Module Inputs

All inputs relevant to the sensor module are provided interactively by the user. However, to free the user from having to input all sensor parameters each time the simulation is run, a sensor characteristic library feature has been implemented. Using this feature, the user may recall any previously defined sensor definition and then use it or edit it as desired. Similarly, the active sensor definition may be saved in the library for future use.

The complete set of sensor menus is illustrated in Figure 3-3. There are several SENSOR MENU options which alter the active sensor definition. The T option causes the TRANSFER FUNCTION MENU to be displayed. From this menu, the transfer functions used to model the active sensor may be individually selected. Alternatively, a default selection of transfer function "switch" settings corresponding to any predefined sensor may be loaded from the sensor characteristic library. The C option in the SENSOR MENU affords access to the SENSOR CHARACTERISTIC MENU. The L and A options in this menu control access to the sensor characteristic library. A special option switch S controls the use of transfer function switch settings stored in the sensor library. If S is false, the transfer function switch table (TRANSFER FUNCTION MENU) is not loaded with the rest of the sensor parameters. Thus, the S option will usually be left in its default true setting. The remaining menu options (D,W,F, and T) select the menus from which sensor parameters are actually input. All the sensor input parameters are listed in Table 3-11; we will briefly comment on each menu in the following subsections.

3.2.1 Detector Characteristic Menu

The inputs required by this menu are relatively straight forward. Note that the detector area is required only for noise calculations, and that the focal length input units are millimeters. Also note that options P and S need only be selected if the optical system blur and/or the LED transfer functions are used. All other parameters must be entered in all cases.

Table 3-11. Interactive Inputs to the Sensor Module

Menu Name	Menu Option	Variable Name	Variable Description
Detector Characteristic Menu			
	A	AD	Area of a single detector element (cm^2)
	F	FN	f/# of the optical system
	L	FL	Focal length of the optical system (mm)
	P	W	e^{-1} half width of the optical system point spread function (mrad)
	I	IFOVX,IFOVY	Sensor instantaneous field-of-view in the along-scan and cross-scan dimensions (mrad)
	V	FOVX,FOVY	Sensor field-of-view in the along-scan and cross-scan dimensions (mrad)
	S	XX,XY	Size of the LEDs in the E-O multiplexer; along-scan and cross-scan dimensions respectively (mrad)

Table 3-11. Interactive Inputs to the Sensor Module (continued)

Menu Name	Menu Option	Variable Name	Variable Description
Spectral Characteristic Menu			
	W	WAVE1,WAVE2	Lower and upper limits of the sensor spectral bandpass (microns)
	N	NL	Number of discrete wavelengths at which the sensor spectral characteristics are to be specified (2-10)
	D	DPEAK	Peak detector specific detectivity (D*) within the spectral band defined by array LAM (cm-(Hz)$^{1/2}$/W)
	C	WAVED	Wavelength at which optical system diffraction calculations are performed, usually the center of the sensor bandpass (microns)
	A	LAM(I)	Array of length NL which contains the wavelengths where sensor spectral characterictics are defined (microns)
	S	DWAVE (I)	Array of length NL which contains the detector spectral D* characteristics normalized by DPEAK (0-1)

Table 3-11. Interactive Inputs to the Sensor Module (continued)

Menu Name	Menu Option	Variable Name	Variable Description
	T	TO	Array of length NL which contains the optical system spectral transmittance (0-1)
Frequency Characteristic Menu			
	D	FD	Detector 3-db cut-off frequency (Hz)
	R	FR	Sensor frame rate (Hz)
	O	NOV	Sensor overscan ratio
	S	NSC	Sensor scan efficiency (0-1)
	N	NP,NS	Number of parallel (cross-scan) and serial (along-scan) detectors
	E	FLP,FHP	3-db frequencies of single pole lowpass and highpass electronic filters (Hz)
	M	FMAX	Frequency at which the maximum electronic boost is applied (Hz)
	B	BB	Boost amplitude at FMAX
	Y	FNYQ	Nyquist frequency limit in the along-scan dimension caused by electronic multiplexing (Hz)

Table 3-11. Interactive Inputs to the Sensor Module (continued)

Menu Name	Menu Option	Variable Name	Variable Description
	P	DDX,DDY	Along-scan and cross-scan stabilization transfer function parameters ($mrad^2$)
	A	XLIM,YLIM	Highest spatial frequency in the along-scan and cross-scan dimensions at which inverse transfer functions are applied ($mrad^{-1}$)
Tabular MTF Inputs	N	NSP	Number of discrete spatial frequencies at which tabular sensor MTFs will be specified (2-10)
	F	SPFRQ(I)	Array of length NSP containing the spatial frequencies at which sensor MTFs will be input ($mrad^{-1}$)
	O	OMTF(I)	Array of length NSP containing the radially symetric optical system MTF (0-1)
	V,C	VMTFX(I), VMTFY(I)	Arrays containing the along-scan and cross-scan vidicon MTF (0-1)
	S,M	SMTFX(I), SMTFY(I)	Arrays containing the along-scan and cross-scan stabilization MTF (0-1)

3.2.2 Spectral Characteristics Menu

There are no optional inputs in this menu. A particularly important parameter is the detector D*. This parameter depends on spectral wavelength and temporal frequency. The desired input is the D* at the wavelength of peak spectral response, and corresponding to a temporal frequency that is between the 1/f detector noise region and the detector cut-off frequency. Note that the current version of the sensor model assumes that the detector noise is white within the modeled sensor's electrical bandpass. Finally, note that DWAVE must equal 1.0 at the wavelength where DPEAK applies.

3.2.3 Frequency Characteristic Menu

Many of the inputs allowed by this menu are optional. The following menu options must be selected only if the corresponding transfer function is required:

Menu Option	Transfer Function
D	Detector - Temporal
E	Electronics
M,B	Boost
Y	Along-scan Sampling
P	Stabilization - Formula

Finally, note that the A option allows limits to be input which are used when the I option (Invert Transfer Functions) of the SENSOR MENU is selected. The limits are required to prevent excesssive noise amplification when performing aperture corrections on measured data.

3.2.4 Tabular MTF Inputs

All of the inputs requested by this menu are optional. The appropriate inputs are required only if the corresponding tabular transfer function is to be used in the sensor definition.

3.3 Atmospheric Effects Module

The atmospheric effects module incorporated in the simulation is based on the LOWTRAN6 code. Major modifications to the code include the following:

1. Simplification of geometry inputs to limit the line of sight to a horizontal (constant-pressure) path.

2. Replacement of all input cards with a menu-driven calling routine.

3. Elimination of the Navy maritime aerosol module.

4. Elimination of the vertical structure algorithm.

5. Deleting all input/output statements within the code.

6. Elimination of the cirrus cloud model.

7. Limiting stratospheric and upper atmospheric profiles to default types.

8. Eliminating the option of the user to input a user-defined layered atmosphere. The user may still input horizontal path parameters or a standard model atmosphere.

9. Defaults are automatically provided for all inputs.

The following features of LOWTRAN6 were retained in the model:

1. Scattering of solar radiation into the line of sight.

2. Updated water vapor continuum absorption.

3. Relative humidity-dependent aerosol profiles.

4. Absorption and scattering due to rain.

5. Scattering of radiation from the ground into the line of sight.

6. Calculations may be made at any wavelength from .25 μm to 28 μm.

3.3.1. Methods of Operation of the Atmospheric Effects Module

The atmospheric effects module treats natural obscuration as being spatially homogeneous across the scene, depending only on range. In the present version of the simulation, the background and target are treated as being at the same

range. This will be modified in the next version to allow separate background and target images to be combined at different ranges from the observer.

There are two different modes of operation of the atmospheric effects module in the current version of the simulation. The first mode is for the atmospheric effects module to be called explicitly by the user from the main menu. This will, in general, need to be done at least once whenever the simulation is run in order to set up the meteorological conditions, geometry parameters, and wavelengths at which calculations are to be performed. After setting up the inputs, the user can either perform the LOWTRAN calculations to modify the scene radiance map or return to the main menu to execute the battlefield effects module.

The atmospheric effects module may also be called implicitly from the battlefield effects module. In this mode, the atmospheric effects module is called automatically and the user has no opportunity to modify input parameters after the battlefield effects module begins to perform calculations. The battlefield effects module calls the atmospheric effects module twice, to compute transmittance and radiance for the atmospheric path between the target and the smoke cloud, and the path between the smoke cloud and the observer. The range used in the atmospheric effects module is passed directly from the battlefield effects module based on its calculation of smoke cloud location. This range is independent of the range which is input by the user in the atmospheric effects module path geometry menu. If the atmospheric effects module is called explicitly later in the same run, the user-input range, rather than the range last passsed by the battlefield effects module, will be used in the calculations.

3.3.2 Atmospheric Effects Module Inputs

The original LOWTRAN6 code required the user to specify 31 input parameters, with another 36 input parameters required if certain options were selected by the user. The modified version of LOWTRAN6 included in the atmospheric effects module requires only 14 input variables, with three other variables optional if the user wishes to specify horizontal path parameters. Defaults are available for all input variables. All input variables may be input from the atmospheric effects menu or one of the other menus called by the atmospheric effects menu.

Table 3-12 describes the variables which may be input from each of the menus in the atmospheric effects module. Every

Table 3-12. Description of Options and Input Variables which may be Accessed through Menus in the Atmospheric Effects Module (continued)

Menu Name	Option	LOWTRAN6 Input Variables Entered	Description
Atmospheric Effects Menu			
	M		Select meteorological parameter menu
	P		Select path geometry menu
	W	V1,V2,DV	Enter starting wavenumber, ending wavenumber, and wavenumber increment for calculations
	C		Calculate transmittance and radiance using LOWTRAN6
	Q		Return to main menu without performing calculations
Meteorological Parameter Menu			
	A	MODEL*	Choose a model atmosphere
	H	IHAZE	Choose an aerosol model
	V	VIS	Enter visibility (km)
	R	RAINRT	Enter rain rate (mm/hr)
	C		Enter refractive index structure constant (not used by LOWTRAN6, but used by sensor module)
	D		Return to default values for meteorological inputs
	Q		Return to Atmospheric Effects Menu

Table 3-12. Description of Options and Input Variables which may be Accessed through Menus in the Atmospheric Effects Module.

Menu Name	Option	LOWTRAN6 Input Variables Entered	Description
Path Geometry Menu			
	H	H1	Enter height above ground
	R	RANGE	Enter range of path
	J	IDAY	Enter Julian day
	T	TIME	Enter time of day
	L	PARM1	Enter site latitude
	A	PARM2	Enter site longitude
	P	PSIPO	Enter path angle (0=facing north, 90 = east)
	D		Return to default values for path geometry inputs
	Q		Return to Atmospheric Effects Menu

* The values for P, T and RH are entered by the user after the appropriate prompts if MODEL = 0 (user-supplied path parameters) is selected.

effort has been made to make it easy for the user to select the appropriate parameters for the desired scenario. The appropriate units for the quantities to be entered are included in the prompts. If further information concerning inputs is required, the user is advised to consult the instructions for using LOWTRAN6 [1].

For the user who is already familiar with LOWTRAN6 inputs, Table 3-13 describes which of the LOWTRAN6 inputs are required by the model, which are automatically set by the model, and which options have been eliminated. Default values for all inputs are provided in this table.

3.4 Battlefield Effects Module Inputs

The battlefield effects module obtains inputs both interactively from the user, and from a card image input list. All of the interactive inputs are found in the Battlefield Effects Menu, and concern the overall scenario geometry. The sole purpose of the interactive inputs is to allow the user to specify any arbitrary observer-target viewing geometry easily, without re-defining the deployment of obscurant sources. Information concerning specification of the scenario geometry can be found in section 3.1.4.

The card image input list must be prepared prior to running the simulation. Each card image is read using the FORTRAN format (2A2,6x,7F10.3). The name positioned in the first columns of each "card" identifies the type of information contained in that record; the card order is generally unimportant. Table 3-14 lists the parameters which are input on each card. While all these parameters are defined in referenced reports [2,3,4], we will comment briefly on each card type in the following subsections.

REFD

The REFD card contains geometry and meteorological reference quantities. The variable PHNOR is required to define the relation between the scenario coordinate system and the compass headings used to define wind direction. The parameter ZR defines the terrain roughness and thereby influences the obscurant vertical transport. Pasquill [11] discusses this parameter, however the following table is provided for easy reference:

Table 3-13. LOWTRAN6 Inputs and Defaults used in Atmospheric Effects Module (continued)

Card Name	Variable Name	Code *	Default	Comments
CARD1	MODEL	R	2 (Mid-latitude summer)	Model = 7 not permitted
	ITYPE	A	1	Horizontal path only
	IEMSCT	A	2	
	M1	A	0	
	M2	A	0	
	M3	A	0	
	IM	E		
	NOPRT	E		
	TBOUND	A	0	Based on model atmosphere
	SALB	A	0.5	
CARD2	IHAZE	R	1(Rural)	Maritime aerosol not permitted
	ISEASN	A	0	Based on model atmosphere
	IVULCN	A	0	
	ICSTL	E		
	ICIR	E		
	IVSA	E		
	VIS	R	23.	
	WSS	E		
	WHH	E		
	RAINRT	R	0.	
CARD2A		E		All variables eliminated
CARD2B		E		All variables eliminated
CARD2C1		E		All variables eliminated
CARD2D		E		All variables eliminated
CARD3	H1	R	0.01	
	H2	E		
	ANGLE	E		
	RANGE	R	1.0	
	BETA	E		
	RO	A	0.	Based on model atmosphere
	LEN	E		

Table 3-13. LOWTRAN6 Inputs and Defaults used in Atmospheric Effects Module.

Card Name	Variable Name	Code *	Default	Comments
CARD3'	H1	R	0.01	
	P	O	1013.	Only for MODEL = 0
	T	O	25.	Only for MODEL = 0
	DP	E		
	RH	O	70.	Only for MODEL = 0
	WH	E		
	WO	E		
	RANGE	R	1.0	
CARD3A1	IPARM	A	1	
	IPH	A	2	
	IDAY	R	270	
	ISOUR	A	0	
CARD3A2	PARM1	R	43.	
	PARM2	R	106.	
	PARM3	E		
	PARM4	E		
	TIME	R	13.33	
	PSIPO	R	90.	
	ANGLEM	E		
	G	E		
CARD3B1		E		All variables eliminated
CARD3B2		E		All variables eliminated
CARD4	V1	R	800.	
	V2	R	1250.	
	DV	R	20.	
CARD5		E		All variables eliminated

* Code R = Input required
O = Input optional (required only for model = 0)
A = Automatically set (user has no control)
E = Option eliminated

Table 3-14. Card Inputs to the Battlefield Effects Module

Card Name	Variable Name	Variable Description
REFD	PHNOR	North heading measured clockwise from the positive Y axis (degrees)
	WREF	Wind speed reference height (m)
	TREF	Air temperature reference (m)
	ZR	Terrain roughness parameter (cm)
	RC	Terrain scavenging factor (0 to 1)
DETD	WAVE	Calculation wavelength (microns)
SRCL	---	Use one card per smoke source, 12 sources maximum
	RS (#,1)	X-Coordinate of source (m)
	RS (#,2)	Y-Coordinate of source (m)
	RS (#,4)	Time of source burst (s)
	IGREN (#)	Source type: 1.0 = L8A1 grenade, RP 2.0 = XM76 grenade, EA5763 3.0-6.0 = User - defined
MET1	IPAS	Pasquill Stability Category, A-F (1-6)
	HM	Mixing Height (m)
	THM	Mixing height temperature (C)
	TAIR	Air temperature at height, TREF (C)
	GRAD1	Temperature gradient (C/m)
	RH	Relative humidity
	TDEW	Dew Point Temperature (C)

Table 3-14. Card Inputs to the Battlefield Effects Module (continued)

Card Name	Variable Name	Variable Description
MET2	WDPS	Wind speed at height WREF (m/s)
	WDIR	Wind direction at height WREF (degrees)
	WPR	Wind power law exponent
	ESFC	Surface irradiance in a one micron bandpass surrounding WAVE (W/m^2)
	TEM (3)	Ground Temperature (C)
	RFL (3)	Ground reflectivity (0 to 1)
SKYR	SKYRAD (I)	Relative sky sector radiance
SKYA	SKYANG (I,1)	Sky sector zenith angle (degrees)
	SKYANG (I,2)	Sky sector azimuth angle (degrees)
PPSD	PPSFLX (I)	External Source Beam Flux in a one micron bandpass about WAVE (W/m^2)
	PPSANG (I,1)	External Source Zenith angle (degrees)
	PPSANG (I,2)	External Source Azimuth angle (degrees)
PHFD	PHF (I)	Obscurant scattering phase function (1/Sr)
PHAD	PHA (I)	Corresponding scattering angles (degrees)
SMKD	ISMK	Smoke Type: 1.0 = Phosphorus 2.0 = EA5763 3.0-6.0 = User defined non-hygroscopic smoke type

Table 3-14. Card Inputs to the Battlefield Effects Module (continued)

Card Name	Variable Name	Variable Description
	EXT (ISMK)	Obscurant Mass Extinction Coefficient (m^2/g)
	OBAR (ISMK)	Obscurant Single Scattering Albedo
	QH (ISMK)	Obscurant Heat Release (cal/g)
	CP (ISMK)	Obscurant Specific Heat (cal/gm-C)
SRCD	ITYP	Grenade Type: 1.0 = L8A1, Phosphorus 2.0 = XM76, EA5763 3.0-6.0 = User-defined
	RG (ITYP, 1)	Smoke Type: 1.0 = Phosphorus 2.0 = EA5763 3.0-6.0 = User-defined non-hygroscopic smoke
	RG (ITYP, 2)	Munition fill mass (Kg)
	RG (ITYP, 3)	Munition source efficiency (percent)
	RG (ITYP, 4)	- not used -
	RG (ITYP, 11)	Munition Burn Duration (s)
	RG (ITYP, 12)	Munition burst height (m)
SGMA	ITYP	See card SRCD
	RG (ITYP, 5)	Initial Burst X-Sigma (m)
	RG (ITYP, 6)	Initial Burst Y-Sigma (m)
	RG (ITYP, 7)	Initial Burst Z-Sizma (m)
	RG (ITYP, 8)	Ground Source X-Sigma (m)
	RG (ITYP, 9)	Ground Source Y-Sigma (m)
	RG (ITYP, 10)	Ground Source Z-Sigma (m)

Table 3-14. Card Inputs to the Battlefield Effects Module (continued)

Card Name	Variable Name	Variable Description
CNTR	STIME	Scenario start time, usually 0.0 (s)
	ETIME	Scenario end time (s)
	DTIME	Increment between calculation of obscurant transmission and radiance maps (s)
	MODE	Radiance model option: 0.0 = Fast radiance approximation 1.0 = Full sky-sector single scatter radiance model
	NTHE	Number of zenith angle divisions for sky and ground sector calculations
	NPHE	Number of azimuth angle divisions for sky and ground sector calculations
	STEMP	Input obscurant cloud temperature for fast radiance approximation (MODE = 0) (C)
MAD1	MAD	MAD Puff Option Switch 0.0 = ACT II Smoke Transport Methodology 1.0 = MAD Puff Smoke Transport Methodology
	MDMAX	Maximum # of puffs to consider in the MAD Puff Mode (0 < MDMAX < 601)
	NRAND	Odd integer random number seed
	IBUOY	Buoyancy model switch 0.0 = no buoyancy 1.0 = Empirical buoyancy model

Table 3-14. Card Inputs to the Battlefield Effects Module (continued)

Card Name	Variable Name	Variable Description
	MPRINT	Puff data printing switch 0.0 = no printing 1.0 = diagnostic data at each model time step printed on I/O Unit 3
TURB	USTAR	Friction Velocity (m/s)
	SIGU	Lagrangian standard deviation of wind fluctuations, U-component (m/s)
	SIGV	Lagrangian standard deviation of wind fluctuations, V-component (m/s)
	SIGW	Lagrangian standard deviation of wind fluctuations. W-component (m/s)
BURN	ITYP	Munition type code (see card SRCD)
	BN (ITYP, 1)	EO-SAEL Burn Function Coefficient
	BN (ITYP, 2)	EO-SAEL Burn Function Coefficient
	BN (ITYP, 3)	EO-SAEL Burn Function Coefficient
	BN (ITYP, 4)	EO-SAEL Burn Function Coefficient
	BN (ITYP, 5)	EO-SAEL Burn Function Coefficient
	BN (ITYP, 6)	EO-SAEL Burn Function Coefficient
GOGO		Card signals the battlefield module to begin computations
DONE		Card causes the termination of battlefield module computations

ZR (cm)	Terrain Type
0.1	Open sand or smooth water
1.0	Short clipped grass in smooth terrain
10.0	Open grass field or agricultural complex
100.0	Forested or urban environment

Finally, the terrain scavenging factor RC describes how much of the obscurant material which contacts the ground is "reflected" back into the air. The terrain is a perfect reflector if RC=1.

DETD

The card DETD contains only a single input, the wavelength at which transmittance and radiance calculations are performed.

SRCL

Each SRCL card defines the position, burst time, and munition type for a single obscurant source. Up to 12 separate sources may be specified. Note that the coordinate system is identical to that used to interactively specify target and observer positions in the simulation itself. Also, note that two munition type identification codes are reserved for pre-defined vehicle self-screening grenade types.

MET1 and MET2

Most of the basic meteorological quantities which influence the obscurant transport and diffusion are input on these two cards. Note that either the relative humidity or the dew point temperature may be specified. The parameter WPR is used to specify the vertical wind speed profile according to a power law expression of the form:

$$U(z) = U(z_{ref}) \left(\frac{z}{z_{ref}}\right)^{WPR} \qquad (10)$$

where U is the wind speed, z is the height above the ground, and z_{ref} is a reference height.

Perhaps the most difficult parameter to specify is the in-band surface irradiance ESFC. This parameter is the net irradiance from the sky hemisphere in a one micron bandpass centered about WAVE excluding contributions from all point sources such as the sun or moon. Finally, note that if the ground is considered to be a black body, then the ground reflectivity (RFL(3)) should be set to 0.0.

SKYR and SKYA

These cards are used to specify the relative radiance seen looking at different points in the sky hemisphere. The radiance at up to 42 angular positions may be specified. Up to seven radiance values may be input on a single SKYR card; three angular positions may be input on each SKYA card. Of course, the order of angular and radiance inputs is critical so that the correspondence between input pairs is maintained. Note that the absolute magnitude of the SKYR inputs is of no consequence. The program automatically scales the integral of the diffuse sky hemisphere radiance to equal the surface irradiance ESFC.

PPSD

Up to 2 PPSD cards may be used to define point sources of radiation. The parameter PPSFLX is the surface irradiance in a one micron bandpass centered about WAVE due to a point source at the specified angular position.

PHFD and PHAD

These cards are used to input the scattering phase function of the obscurant media. Up to 70 phase function values may be input on PHFD cards (7 per card) while the corresponding scattering angles are input on PHAD cards. Only one phase function may be input; it is used to describe the scattering from all obscurant materials relevant to a scenario. Therefore, although any number of different absorbing media may be considered in a single scenario, only a single scattering media may be correctly considered.

SMKD

This card defines the relevant properties of the obscurant material. Note that for the predefined smoke materials (phosphorus smoke and EA5763), only the two optical parameters applicable to the wavelength of interest (WAVE) must be input. The parameter QH quantifies the amount of heat imparted to the obscurant cloud in its formation; it is used to calculate the cloud temperature and buoyancy. CP is simply the specific heat of the smoke material. Finally, the comment that only non-hygroscopic smokes may be defined by the user refers to the fact that the model does not treat the adsorption, absorption, and condensation reactions for any material other than phosphorus smoke, which is predefined.

SRCD and SGMA

These cards are used to define smoke munition types. Neither card is required if the default grenades (L8A1 or XM76) are the only source types considered. Note that the product of the input munition fill mass and the munition source efficiency is assumed to equal the total mass of lofted obscurant material produced by the source. The munition source efficiency may be set greater than 100% if the yield factor of a user-defined hygroscopic smoke is to be artificially included. Also, note that the munition burn duration (RG (ITYP,11)) is described in conjunction with inputs provided on the BURN card.

The inputs on the SGMA card refer to the initial spatial distribution of smoke produced by the munition. A three dimensional gaussian mass distribution is used to describe the smoke cloud produced by the munition burst, and during each successive modeled time step. The inputs are the standard deviations of these distributions. A single burst puff is generated for each munition. Puffs from source material which is either scattered on the ground or remains in the munition canister are generated at a rate of one per second; the smoke mass contained in each puff is determined by the munition burn function (see card BURN).

CNTR

This card specifies a number of simulation control parameters. Assuming that STIME is specified as 0.0, ETIME determines the time at which the obscurant transmission and radiance map is calculated for use in the simulation scenario. The input DTIME should be set equal to ETIME since the simulation ignores any intermediate radiance map calculations.

The MODE input selects whether the full single scatter radiative transfer solution is used. In the fast radiance mode, the smoke cloud temperature must be input using the variable STEMP. Further, the obscurant cloud is treated as a diffuse reflector. When MODE is set to 1.0, the smoke temperatures are calculated by the model so STEMP need not be specified. However, the angular resolution for the sky sector radiance calculations must be specified. The number of sectors considered is the product of NTHE and NPHI.

MAD1

This card allows either the MAD PUFF or the ACT II transport and diffusion methodology to be selected.

TURB

This card allows parameters relevant to the MAD PUFF transport and diffusion methodology to be input. If it is not known, the friction velocity may be computed using the following expression:

$$USTAR = U(z)*k/(\ln(z/ZR)) \tag{11}$$

where U is wind speed, z is height, k is von Karman's number (about 0.4), and ZR is the terrain roughness parameter input on card REFD. This formula assumes that the vertical wind profile is roughly logarithmic. The remaining variables describe the turbulence velocity fluctuations seen by an observer moving with the mean wind. They may be calculated as follows:

$$\begin{aligned} SIGU &= SIG_{az} * U \\ SIGV &= SIGU \\ SIGW &= SIG_{el} * U \end{aligned} \tag{12}$$

where SIG_{az} and SIG_{el} are the standard deviation of angular wind fluctuations measured in radians.

BURN

The BURN card allows the user to define the rate at which a munition produces smoke. The EO SAEL [23] burn function form is used:

$$M(t) = B_1\left(\frac{t}{T_b}\right) + \frac{1}{2} B_2 \left(\frac{t}{T_b}\right)^2 + \frac{1}{3} B_3 \left(\frac{t}{T_b}\right)^3 + \frac{1}{4} B_4 \left(\frac{t}{T_b}\right)^4 + B_5 \left(1.0 - e^{-B_6 t}\right) \tag{13}$$

where B_n are the six coefficients, T_b is the munition burn duration input on card SRCD, and M(T) is proportional to the cumulative amount of smoke produced between t=0 and t=T. For convenience, the program normalizes the burn function so that the user need only supply the correct relative weights of the coefficients; the absolute magnitude of the coefficients is of no importance. Note the EO SAEL documentation [23] provides a convenient source of burn function definitions for a wide variety of inventory and experimental munitions.

Finally, it should be noted that a burn function must be input even for the predefined munition types (L8A1 and XM76). For convenience, we list burn functions for these munitions below:

Munition	Burn Duration(s)	B1	B2	B3	B4	B5	B6
L8A1	360.0	0.6	-0.4	0.0	0.0	0.15	0.30
XM76	1.0	0.0	0.0	0.0	0.0	1.0	999.

GOGO and DONE

The GOGO card should be placed following the last data input card; it signals the program to begin the smoke calculations. The last card in the input deck should be the DONE card. This causes the battlefield module to return control to the ISSM after it completes its calculations. If a DONE card is not present, the smoke model expects to see a new input deck for use in an additional calculation. Since the current version of ISSM only makes use of the last calculation performed by the smoke model, this facility for repetitive calculations has no practical utility at this time.

4.0 Preliminary Model Validation Results

To date, there has been no attempt to validate the simulation as a whole, although this is planned in the future. However, a preliminary attempt has been made to verify the accuracy of the modules of which the simulation is composed. In the case of the sensor module, we present a comparison between the measured and simulated performance of a current technology thermal imaging sensor. Although the comparison is quite favorable, a considerably more thorough effort is required in order to truly validate the model.

In the case of the atmospheric effects models, we have not undertaken any effort to compare the modeled results with measured data. Since the natural and battlefield effects modules have been developed and tested previously, we have merely verified that their performance in the simulation matches the output of the original models.

4.1 Sensor Model Validation

In order to provide a preliminary indication of the sensor model validity, we have predicted the Minimum Resolvable Temperature (MRT) characteristic of an existing sensor for which both measured data and detailed modeling information exist. The sensor we have modeled is a pre-production evaluation version of the TADS thermal imaging sensor. Reference 24, which is an unpublished document prepared by the Martin Marietta Corp., provides measured data, and NVL Static Performance Model inputs which describe the sensor.

The simulation was exercised using the referenced input data to model a sensor viewing a standard 4-bar MRT target presented against a uniform background. We ran the simulation for a matrix of cases which included five bar pattern spatial frequencies and a number of target contrast signature levels. The resulting set of images were then presented to a group of 9 observers. Within each set of images at a particular spatial frequency, the observers were asked to select the lowest contrast signature image in which they could both detect and resolve the MRT pattern. The observers were allowed to optimize the displayed contrast of each image, just as would be the case in a real MRT test. Also, the observers were allowed to adjust their viewing position in any way they desired.

The results of the test are summarized in Table 4-1. Note that there is a variation among the observers at all spatial frequencies except for the lowest. In this case, no observer could detect the bar target with a signature 2.4 times the

Table 4-1. Minimum Resolvable Temperature (MRT) Simulation Test Results.

Spatial Frequency	Ratio of Simulation Observer MRTs to Measured System MRT									Ratio of Observer Average MRT to Measured System MRT	Ratio of NVL Predicted MRT to Measured System MRT
	1	2	3	4	5	6	7	8	9		
0.125 F_o	4.8*	4.8*	4.8*	4.8*	4.8*	4.8*	4.8*	4.8*	4.8*	4.8*	---**
0.37 F_o	1.1	0.8	0.8	1.1	1.1	0.8	1.1	0.8	1.1	0.936	0.253
0.46 F_o	1.0	0.7	0.8	1.0	1.0	1.0	0.8	0.7	1.2	0.907	0.283
0.56 F_o	0.8	0.8	0.8	1.0	1.0	0.8	0.8	0.8	1.0	0.844	0.481
0.65 F_o	1.1	0.6	0.8	1.1	1.1	1.1	0.8	0.8	0.8	0.910	0.724

* Ratio of observer MRT to NVL predicted MRT.
** Measured system MRT not available.

NVL predicted MRT while the target with a signature 4.8 times the NVL predicted MRT was clearly visible to everyone. Interestingly, the predictions based on observer responses compare very favorably with the measured data. Further, predictions made using the NVL Static Performance Model directly seem to be in relatively less agreement with the measured data. However, while the results of this preliminary test are certainly interesting, they cannot be considered a sufficient basis for drawing any conclusions; they merely suggest that future validation attempts will likely prove fruitful.

4.2 Validation of the Atmospheric Effects Module

Validation of the atmospheric effects module was performed by running the module to duplicate the test cases for horizontal (constant pressure) paths designated as Case 3 in the LOWTRAN5 manual [10] and Case 4 in the LOWTRAN6 manual [1]. A comparison of results is presented in Figures 4-1 and 4-2.

The atmospheric effects module was also run to simulate the conditions used to produce Figures 40 and 41 in the LOWTRAN5 manual. These transmittance spectra demonstrate the sensitivity of the model to variations in the type of aerosol present. A comparison between haze models is presented in Figure 4-3, while a comparison of transmittance using the advection and radiation fog models is presented in Figure 4-5. The corresponding figures from the LOWTRAN5 manual are reproduced as Figures 4-4 and 4-6.

As can be seen, the atmospheric effects module duplicates LOWTRAN6 results to within the precision limits of the calculations. The validation efforts presented above do not validate the LOWTRAN6 model, however, but only demonstrate that the modifications to LOWTRAN6 did not affect the results of the calculations.

Perhaps the most important deficiency in the LOWTRAN code is its inability to consider scattering of radiation from all sources into the line of sight. In the case of a dense aerosol, a considerable amount of radiation may be scattered into the line of sight from the surrounding atmosphere. For long atmospheric paths through a dense aerosol, the path radiance calculated by LOWTRAN6 may actually decrease with increasing distance. This, of course, is physically incorrect. Table 4-2 demonstrates this problem. This table presents the results of calculations for a midlatitude summer atmosphere with a radiation fog having a 0.1 km meteorological range. Calculations are performed at 800 cm^{-1} for ranges of 0.05 km to 10 km. The path radiance actually decreases as the range increases beyond 0.20 km. As transmit-

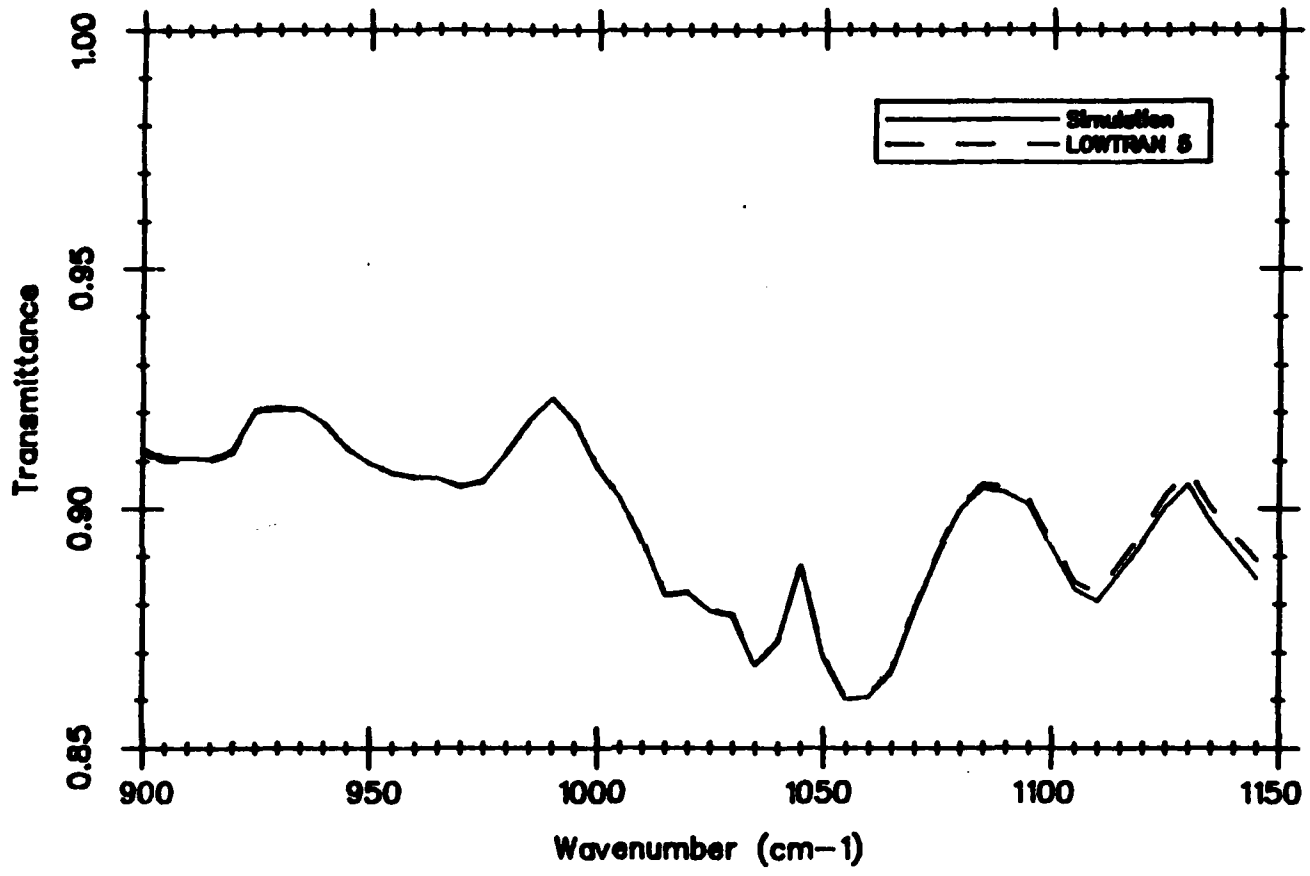

Figure 4-1. Comparison of Transmittance as Calculated by Simulation and Test Case 3 in LOWTRAN5 Manual [10]. Conditions Correspond to a 1-km Horizontal Path at Sea Level, using the US Standard Atmosphere and the Rural, 23 km Visibility Haze.

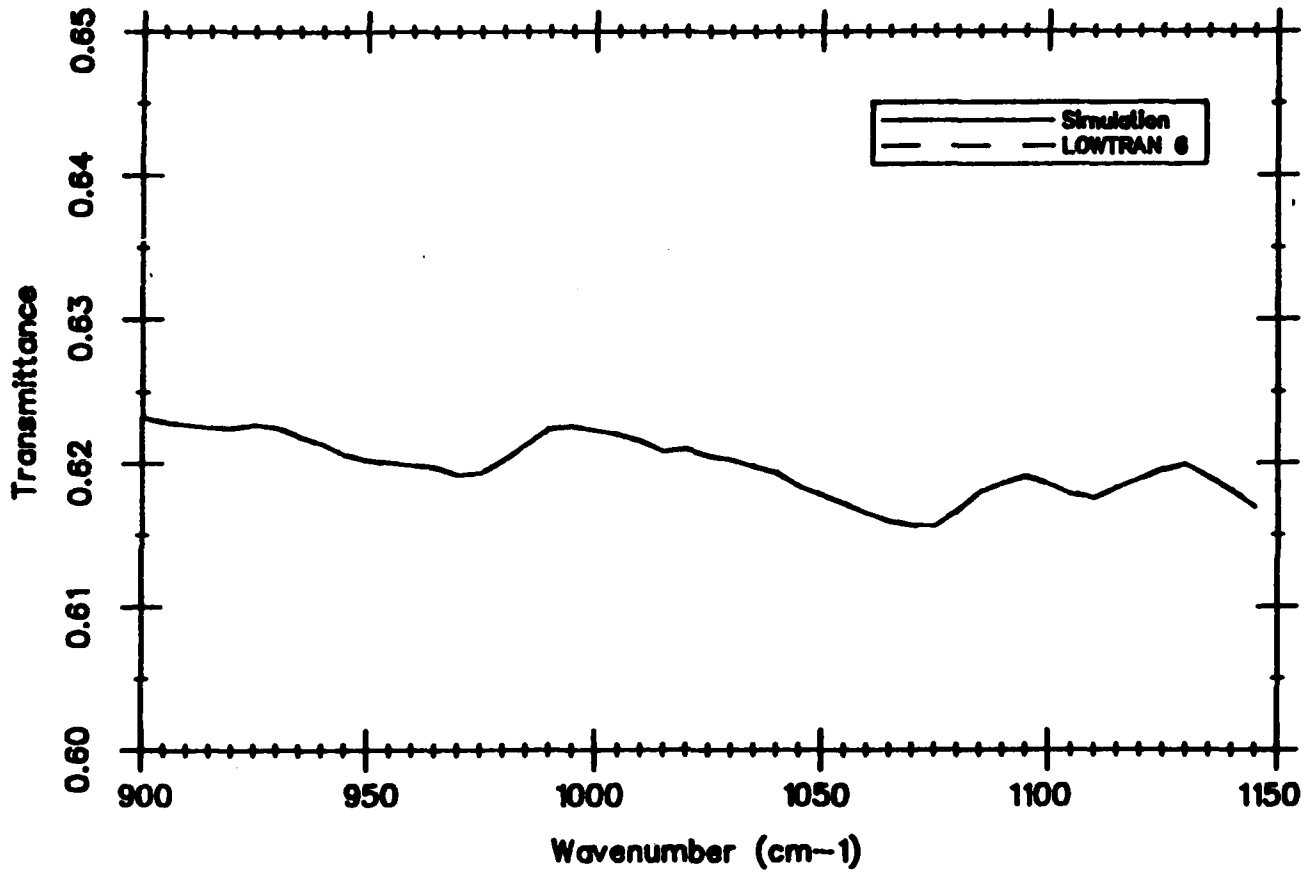

Figure 4-2. Comparison of Transmittance as Calculated by Simulation and Test Case 4 in LOWTRAN6 Manual [1]. Conditions Correspond to a .3 km Path at 0 km Altitude, 23 km Rural Haze, 10 mm/hr Rain.

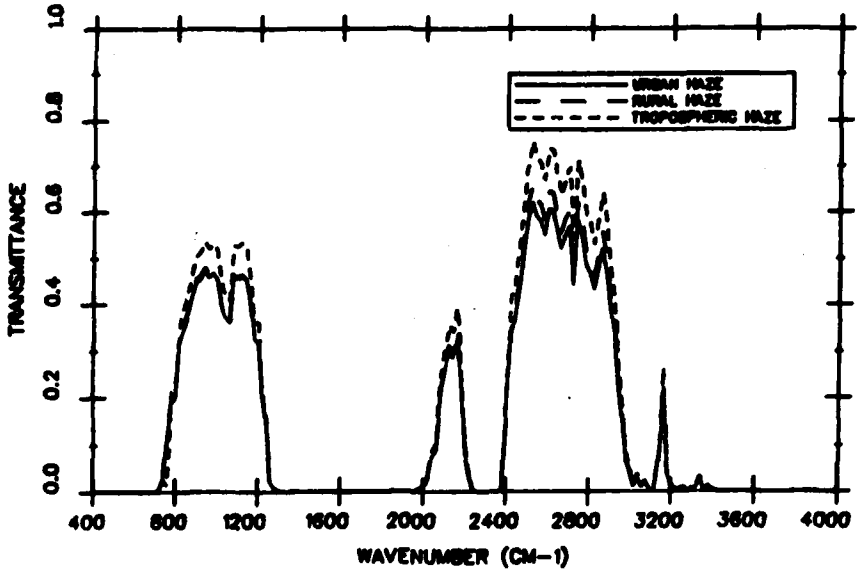

Figure 4-3. Transmittance Spectra through Haze Models Predicted by Simulation

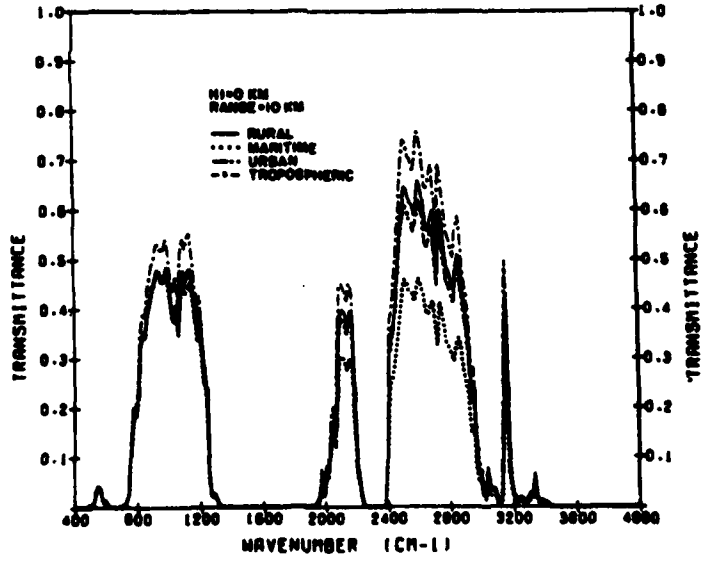

Figure 4-4. Transmittance Spectra for a 10-km Horizontal Path at Sea Level for the Rural, Maritime, Urban, and Tropospheric Aerosol Models using the US Standard Model Atmosphere and a Visibility of 23 km. Calculated by LOWTRAN5 [10].

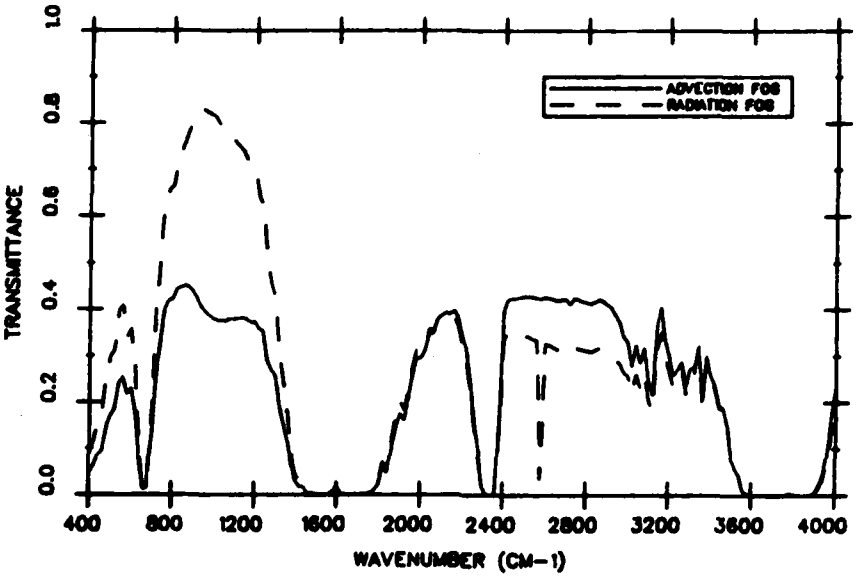

Figure 4-5. Transmittance Spectra through Fog Models used in Simulation

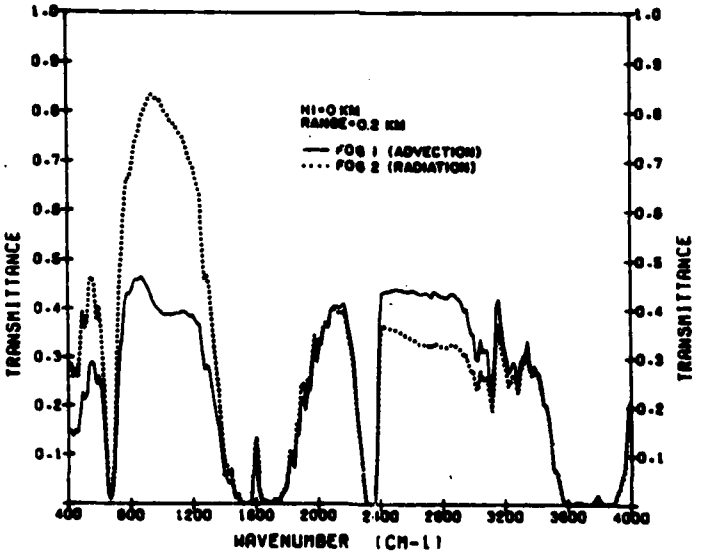

Figure 4-6. Transmittance Spectra for the Advection Fog (Fog 1) and the Radiation Fog (Fog 2) Models, for a 0.2-km Horizontal Path at Sea Level, with the US Standard Model Atmosphere and a 1-km Visibility, from 400 to 4000 cm^{-1}. Calculated by LOWTRAN5 [10].

Table 4-2. Transmittance and Path Radiance as a Function of Range through a Scattering Medium

CONDITIONS: 0.1 km Visibility
Radiation Fog
Midlatitude Summer Model Atmosphere
10 m. Altitude
800 cm^{-1} Wavelength

Range	Transmittance	Path Radiance (W/cm^2-ster-μm)
.05 km	0.4094	6.14×10^{-6}
.10 km	0.1706	8.43×10^{-6}
.15 km	0.0714	9.16×10^{-6}
.20 km	0.0300	9.23×10^{-6}
.30 km	0.0053	8.76×10^{-6}
.40 km	0.0009	8.20×10^{-6}
.50 km	0.0002	7.72×10^{-6}
1.00 km	0.0000	6.58×10^{-6}
2.00 km	0.0000	6.24×10^{-6}
5.00 km	0.0000	6.22×10^{-6}
10.00 km	0.0000	1.24×10^{-5}

tance approaches the machine-limited minimum value around 10^{-39}, path radiance jumps to the correct value.

As a general rule, the atmospheric effects module will not significantly underpredict path radiance if transmittance due to scattering is greater than 10%. If extinction is dominated by absorption rather than scattering (as is the case with most aerosol models in the 8-12 μm region), or if the meteorological range is comparable to or greater than the range of the path, the user can be reasonably confident that path radiance will not be significantly underpredicted.

4.3 Battlefield Module Comparison Runs

The ACTMAD battlefield effects module was exercised in the same manner as LOWTRAN6 in order to verify that the version operating within the simulation provides the same results as known operating versions of the model. Three cases were run which considered both the L8A1 and XM76 default munitions. Both of the radiance calculation options (set using the MODE variable) were used. All runs were made using the MAD PUFF transport and diffusion option.

The result of the comparison was simply that the simulation and the original model versions produce nearly identical results. In cases where the random smoke transport had little effect, the differences in computed values were on the order of 10^{-4} relative to the computed value itself. Note however that since different random number generators are used in the two versions, a comparison is difficult when turbulent transport effects are significant. Nevertheless, we believe the model is functioning properly. Of course, it should be emphasized that there is no evidence to suggest that the battlefield obscuration model is valid for the purpose of incorporating obscurant clouds in observer-interpreted imagery. This type of validation must be left for future efforts.

LIST OF REFERENCES

1 F.X. Kneizys et al., Atmospheric Transmittance/Radiance: Computer Code LOWTRAN6; AFGL-TR-83-0187, Air Force Geophysics Laboratory, August 1983.

2 B.K. Matise et al., Smoke Obscuration Effects Model, OMI-82-025, OptiMetrics, Inc., December 1982.

3 R.A. Sutherland and D.W. Hoock, An Improved Smoke Obscuration Model ACT II: Part I Theory, ASL-TR-0104, U.S. Army Atmospheric Sciences Laboratory, January 1982.

4 F.G. Smith et al., Smoke Obscuration Effects Model, OMI-81-013, OptiMetrics, Inc., November 1981.

5 J.W. Petraska, "The AMGREN Self-Screening Grenade Model", Smoke/Obscurants Symposium VIII, Paper B-16, April 1984.

6 J.A. Ratches et al., Night Laboratory Static Performances Model for Thermal Viewing Systems, ECOM-7043, U.S. Army Night Vision and Electro-Optics Laboratory, April 1975.

7 J.E.A. Selby and R.A. McClatchey, Atmospheric Transmittance from 0.25 to 28.5 μm: Computer Code LOWTRAN2, AFCRL-TR-72-0745, AD A763721, 1972.

8 J.E.A. Selby and R.A. McClatchey, Atmospheric Transmittance from 0.25 to 28.5 μm: Computer Code LOWTRAN3, AFCRL-TR-75-0255, AD A017734, 1975.

9 J.E.A. Selby et al., Atmospheric Transmittance/Radiance: Computer Code LOWTRAN4, AFGL-TR-78-0053, AD A058643, 1978.

10 F.X. Kneizys et al., Atmospheric Transmittance/Radiance: Computer Code LOWTRAN5, AFGL-TR-80-0067, AD A088215, 1980.

11 F. Pasquill, Atmospheric Diffusion, the Dispersion of Windborne Material from Industrial and Other Sources, Ellis Horwood Limited, 1974.

12 S.R. Hanna, "Some Statistics of Lagrangian and Eulerian Wind Fluctuations", Journal of Applied Meteorology 18, pp. 518-525, April 1979.

[13] S.R. Hanna, "A Statistical Diffusion Model for Use with Variable Wind Fields", 4th Symposium on Turbulence, Diffusion, and Air Pollution, American Meteorological Society.

[14] S.R. Hanna, "Lagrangian and Eulerian Time-Scale Relations in the Daytime Boundary Layer", Journal of Applied Meteorology 20, pp. 242-249, March 1981.

[15] L.J. Harding, Numerical Analysis and Applications Software Abstracts, Computing Center Memo 407, 4th Edition, The University of Michigan, September 1979.

[16] E.O. Brigham, The Fast Fourier Transform, Prentice-Hall, 1974.

[17] W.G. Driscoll, Editor, Handbook of Optics, McGraw-Hill Book Company, 1978.

[18] W.L. Wolfe and G.J. Zissis, Editors, The Infrared Handbook, The Infrared Information and Analysis (IRIA) Center, Environmental Research Institute of Michigan, 1978.

[19] D.L. Fried, "Optical Resolution Through a Randomly Inhomogeneous Medium for Very Long and Very Short Exposures", JOSA 56, #10, p.1372, October 1966.

[20] D.L. Fried, "Limiting Resolution Looking Down Through the Atmosphere", JOSA 56, #10, p.1380, October 1966.

[21] D.L. Fried, "Varieties of Isoplanatism", Imaging Through the Atmosphere, SPIE Vol. 75, 1976.

[22] K.E. Kunkel et al., Characterization of Atmospheric Conditions at the High Energy Laser System Test Facility (HELSTF), White Sands Missile Range, New Mexico, August 1977 to October 1978, Part II: Optical Turbulence, Wind, Water Vapor Pressure, Temperature, ASL-TR-0077, U.S. Army Atmospheric Sciences Laboratory, February 1981.

[23] L.D. Duncan, et al., Editors, EOSAEL 82, Vol. III: Transmission Through Battlefield Aerosols, ASL-TR-0122, U.S. Army Atmospheric Sciences Laboratory, November 1983.

[24] TADS System Specifications, NVL Static Performance Model Input Set, designed to simulate the TADS thermal imager. Supplied to the U.S. Army Missile Command by Martin Marietta (TADS contractor) in an unpublished document (CONFIDENTIAL).

DISTRIBUTION LIST

	Copies
Commander US Army Tank-Automotive Command ATTN: AMSTA-TSL (Technical Library) Warren, MI 48397-5000	2
Manager Defense Logistics Studies Information Exchange ATTN: DRXMC-D Fort Lee, VA 23801	2
Commander Defense Technical Information Center Bldg. 5, Cameron Station ATTN: DDAC Alexandria, VA 22314	12

END

FILMED

6-85

DTIC